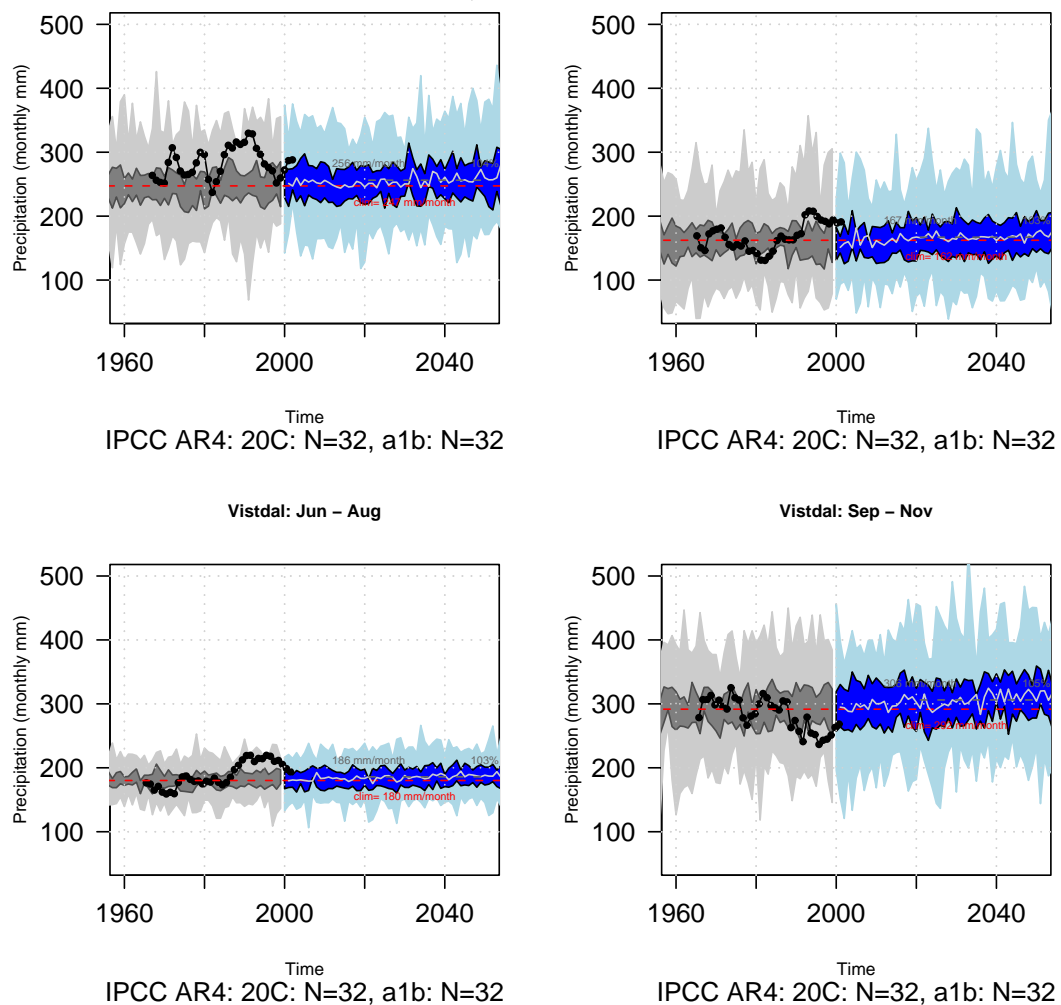




Appendix B


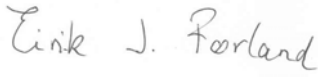
Results from ESD analyses on precipitation representing twenty-five Norwegian catchments

Torill Engen-Skaugen, Rasmus Benestad and Eirik J. Førland



The figure shows the spread of empirically downscaled precipitation with precipitation as predictor from the 32 GCMs used for the historic period 1958 -2000 and the 29 GCMs for the future period 2000-2050 following the SRES A1b emission scenario for Vistdal. Projections are derived for four seasons; winter (upper left), spring (upper right), summer (lower left) and autumn (lower right). Mean temperature for the catchment as a whole, estimated from observations, is drawn as a dotted black curve.

Title Appendix B - Results from ESD analyses on precipitation representing twenty-five Norwegian catchments	Date 08.12.2008
Section Climate	Report no. 23 b 08
Author(s) Torill Engen-Skaugen, Rasmus Benestad and Eirik J. Førland	Classification <input checked="" type="checkbox"/> Free <input type="checkbox"/> Restricted
	ISSN 1503-8025
	e-ISSN 1503-8025
Client(s) EBL Norwegian Electricity Industry Association	Client's reference MKU-1.8_06
Abstract This is an annex report presenting results from empirically downscaled mean monthly precipitation sum representing twenty-five catchments in Norway. The background, precipitation data used and location together with summary and concluding remarks are given in Engen-Skaugen et al. (2008a). Projections established for the catchments in the Norwegian RegClim project are given as well. Results from ESD analyses on temperature for the catchments are given in Annex report C (Engen-Skauge et al., 2008b).	
Keywords Climate change, ESD, precipitation	

Disiplinary signature  _____	Responsible signature  _____
Inger Hanssen-Bauer	Eirik J. Førland

Postal address	Office	Telephone	Telefax	e-mail: met@met.no	Bank account	Swift code
P.O.Box 43, Blindern NO-0313 OSLO Norway	Niels Henrik Abelsvei 40	+47 22 96 30 00	+47 22 96 30 50	Internet: met.no	7694 05 00628	DNBANOKK

1 Background

Mean monthly precipitation sum is downscaled using Empirical-Statistical Downscaling (ESD) methods for twenty-five Norwegian catchments. The work is documented in Engen-Skaugen et al (2008), The present report is an Annex report presenting resulting plots from empirically downscaled precipitation to selected catchments.

Estimates from ~30 GCM runs for the 20th century and ~30 GCM runs for the 21th century from the CMIP3 (IPCC WG1, 2007) are established. The downscaling involved stepwise multiple regression and a common-EOF frame-work, and was performed on monthly mean/total values. Results with discussion from all twenty-five catchments are presented in the present annex report (Section 2). Summary and concluding remarks are given in Engen-Skaugen et al. (2008a).

Results from ESD of precipitation representing twenty-five selected catchments in Norway (Section 2 in Engen-Skaugen et al., 2008) are presented in Section 2. Results on the respective catchments from earlier studies within the Norwegian RegClim project are given in Section 3.

2 Results from ESD of precipitation

The present study is based on 14 different GCMs following the SRES emission scenario A1b. It is based on ~60 global model runs for the 20th and 21st century, however, not all of these GCM results were used; a quality check was implemented that weeded out poorly performing models (See Section 4 in Engen-Skaugen et al, 2008) for more details.

The time period analysed is 1960-2050 where the time period 1960 – 1990 is used as the control period. The downscaling technique used is ESD (Engen-Skaugen et al, 2008 a). Figs. 2.1 - 2.25 shows the model runs; black is used for the period 1958 – 2000 and blue for the period 2000-2050. Dark colours are used for models within the 25 and 75 percentile, while light colours are used for the model runs outside these thresholds.

2.1 Masi

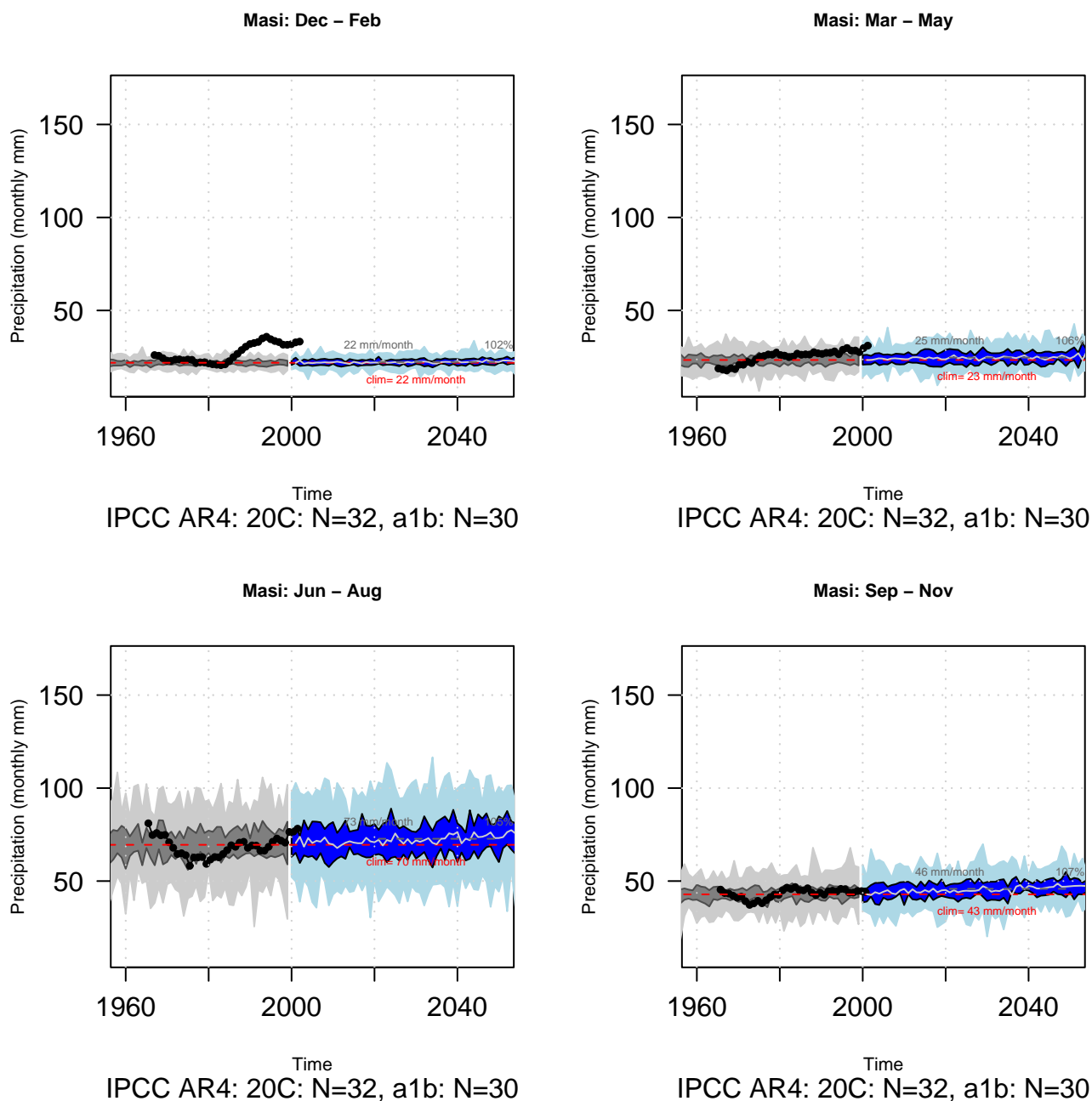


Figure 2.1 The figure shows the spread of empirically downscaled precipitation with precipitation as predictor from the 32 GCMs used for the historic period 1958 -2000 and the 30 GCMs for the future period 2000-2050 following the SRES A1b emission scenario. Projections are derived for four seasons; winter (upper left), spring (upper right), summer (lower left) and autumn (lower right). Mean temperature for the catchment as a whole, estimated from observations, is drawn as a dotted black curve.

2.2 Kobbvatn

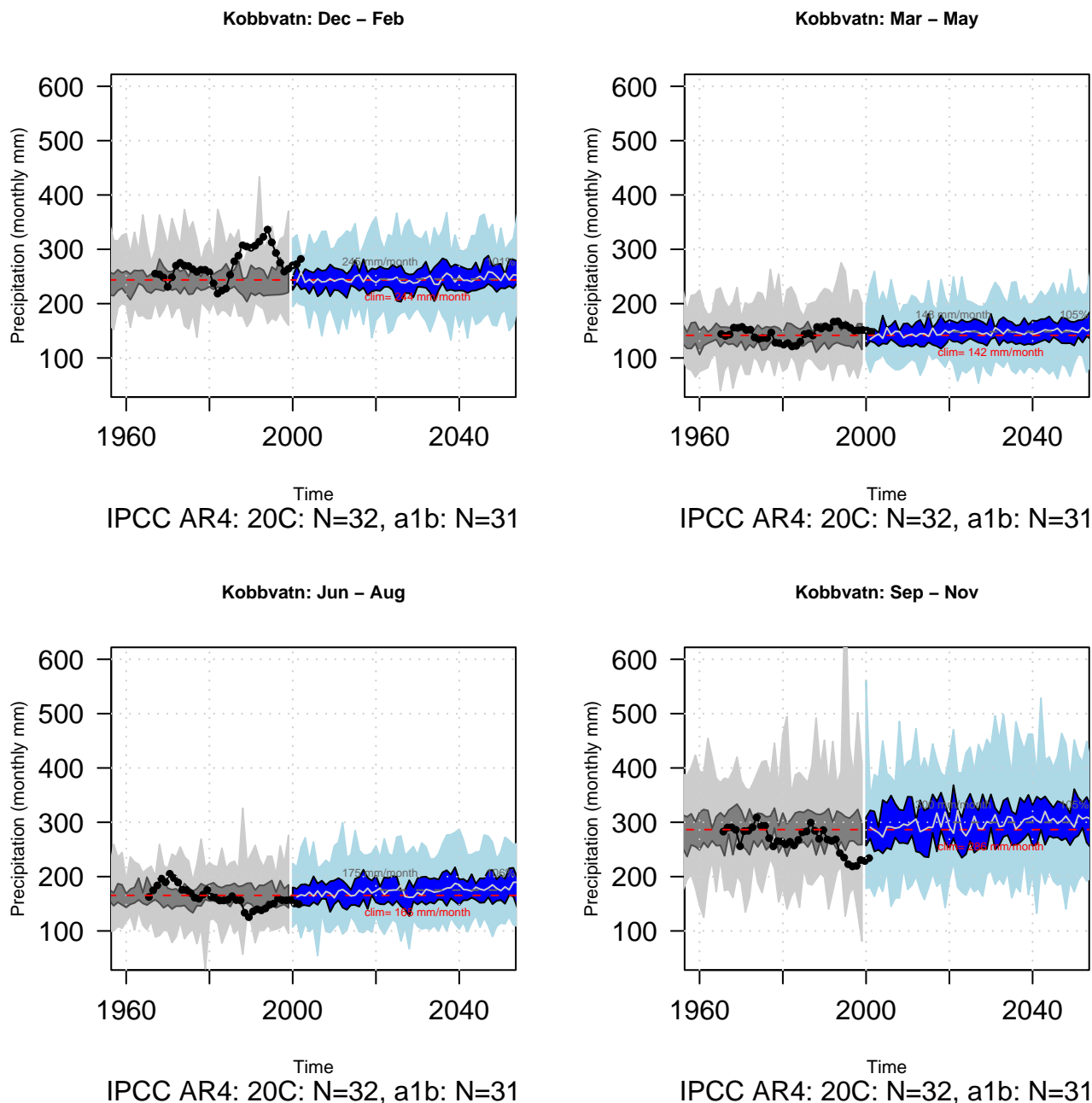


Figure 2.2 The figure shows the spread of empirically downscaled precipitation with precipitation as predictor from the 32 GCMs used for the historic period 1958 -2000 and the 31 GCMs for the future period 2000-2050 following the SRES A1b emission scenario. Projections are derived for four seasons; winter (upper left), spring (upper right), summer (lower left) and autumn (lower right). Mean temperature for the catchment as a whole, estimated from observations, is drawn as a dotted black curve.

2.3 Nervoll

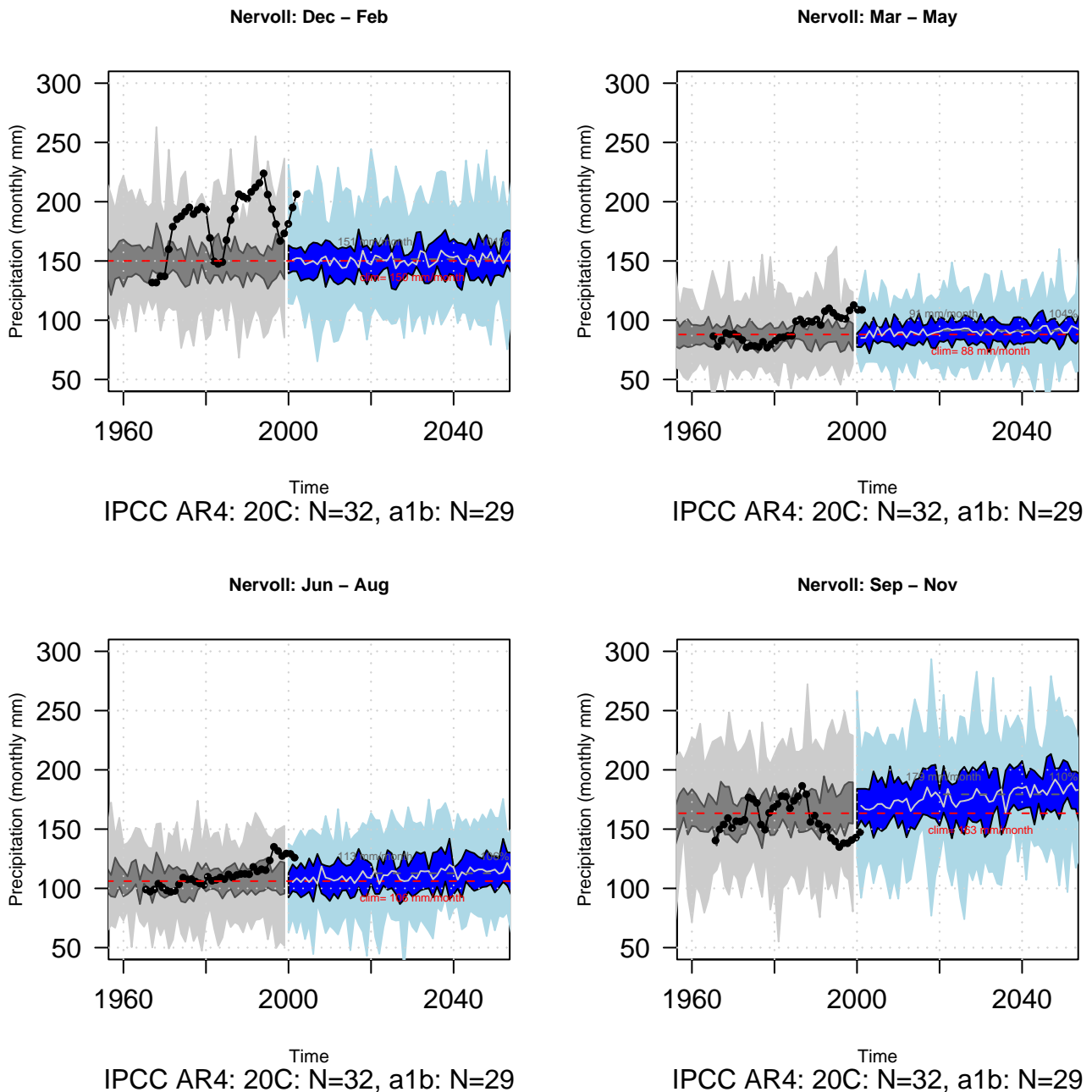


Figure 2.3 The figure shows the spread of empirically downscaled precipitation with precipitation as predictor from the 32 GCMs used for the historic period 1958 -2000 and the 29 GCMs for the future period 2000-2050 following the SRES A1b emission scenario. Projections are derived for four seasons; winter (upper left), spring (upper right), summer (lower left) and autumn (lower right). Mean temperature for the catchment as a whole, estimated from observations, is drawn as a dotted black curve.

2.4 Kjelstad

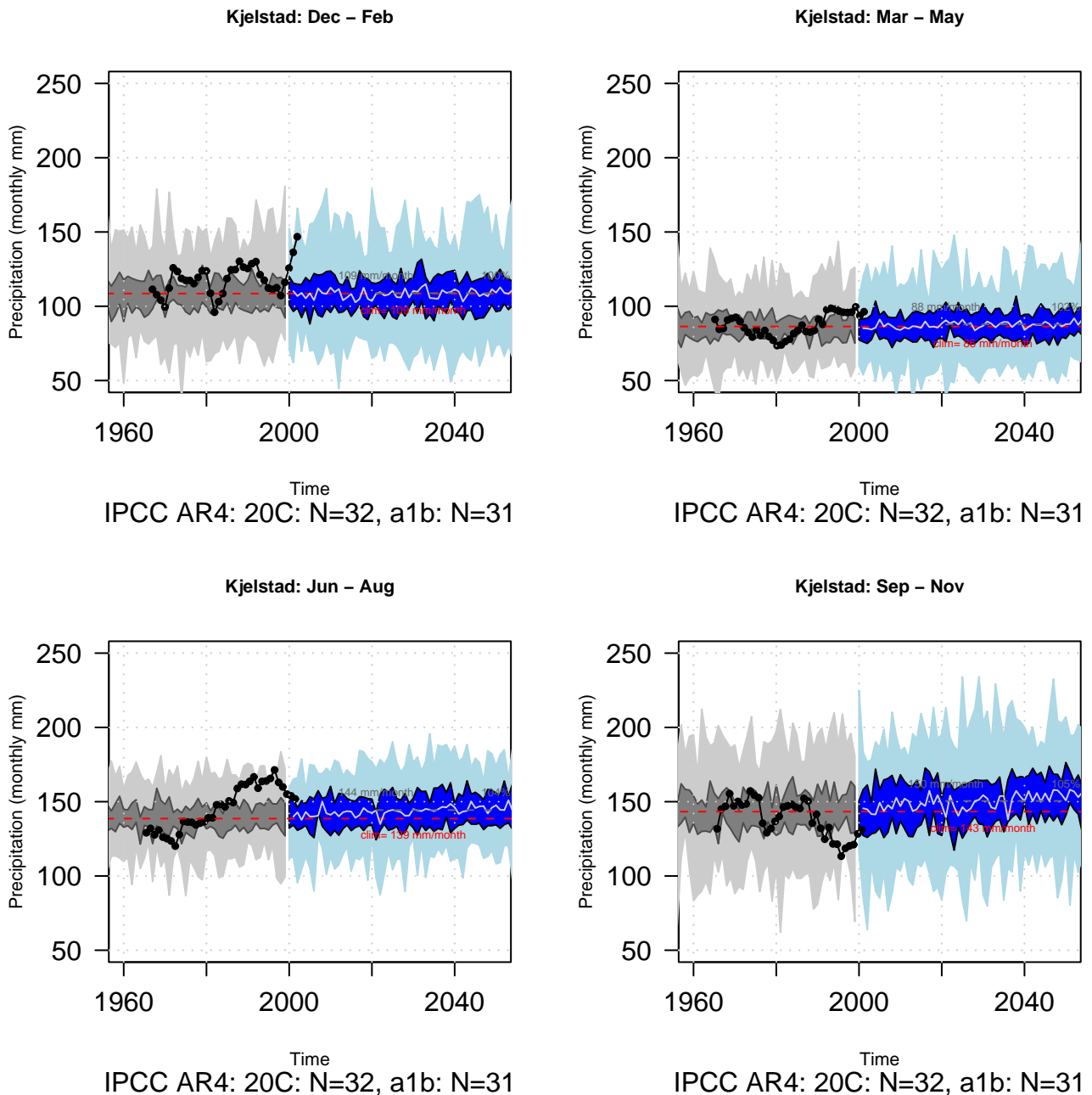


Figure 2.4 The figure shows the spread of empirically downscaled precipitation with precipitation as predictor from the 31 GCMs used for the historic period 1958 -2000 and the 32 GCMs for the future period 2000-2050 following the SRES A1b emission scenario. Projections are derived for four seasons; winter (upper left), spring (upper right), summer (lower left) and autumn (lower right). Mean temperature for the catchment as a whole, estimated from observations, is drawn as a dotted black curve.

2.5 Rathe

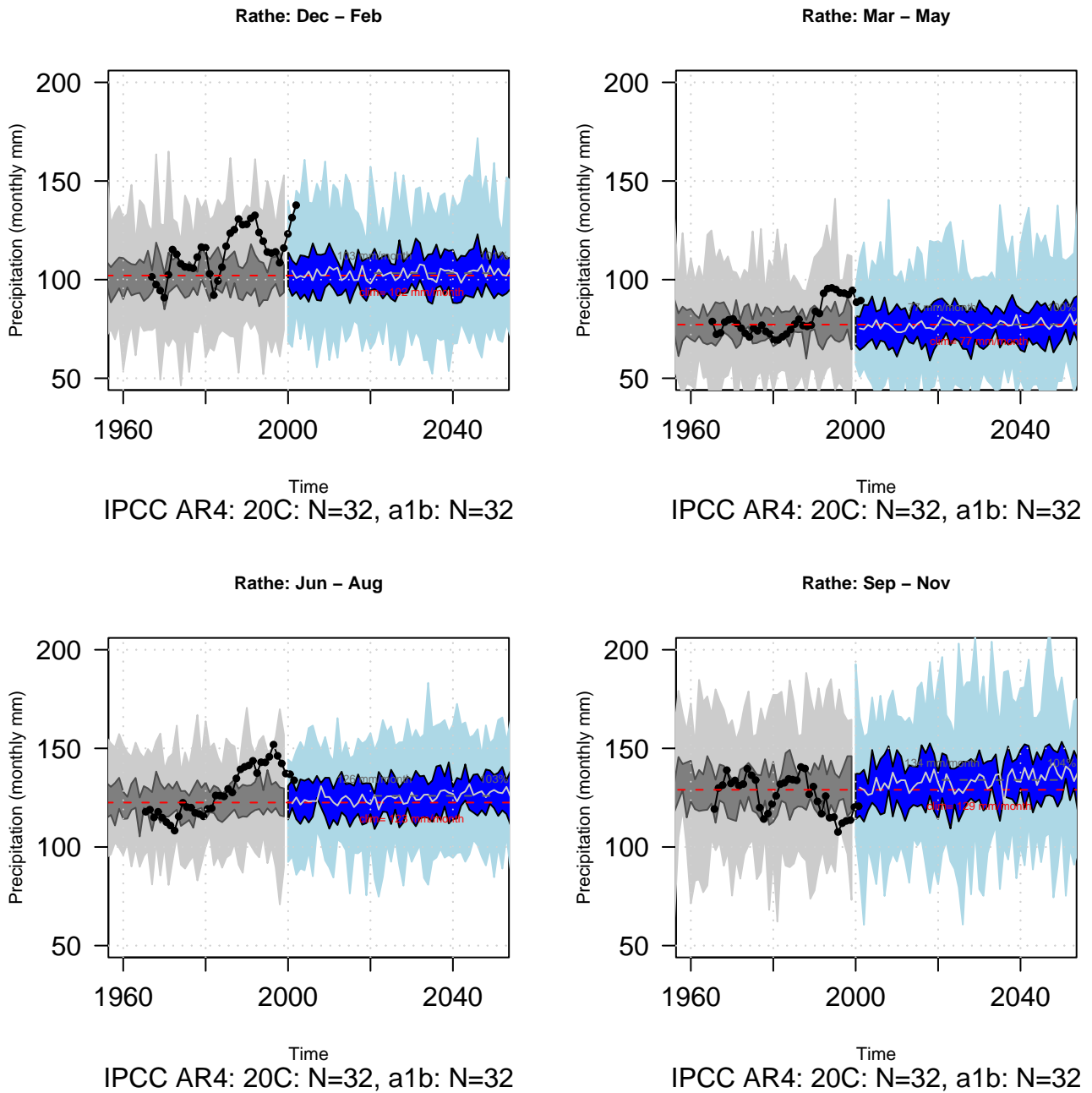


Figure 2.5 The figure shows the spread of empirically downscaled precipitation with precipitation as predictor from the 32 GCMs used for the historic period 1958 -2000 and the 32 GCMs for the future period 2000-2050 following the SRES A1b emission scenario. Projections are derived for four seasons; winter (upper left), spring (upper right), summer (lower left) and autumn (lower right). Mean temperature for the catchment as a whole, estimated from observations, is drawn as a dotted black curve.

2.6 Aursunden

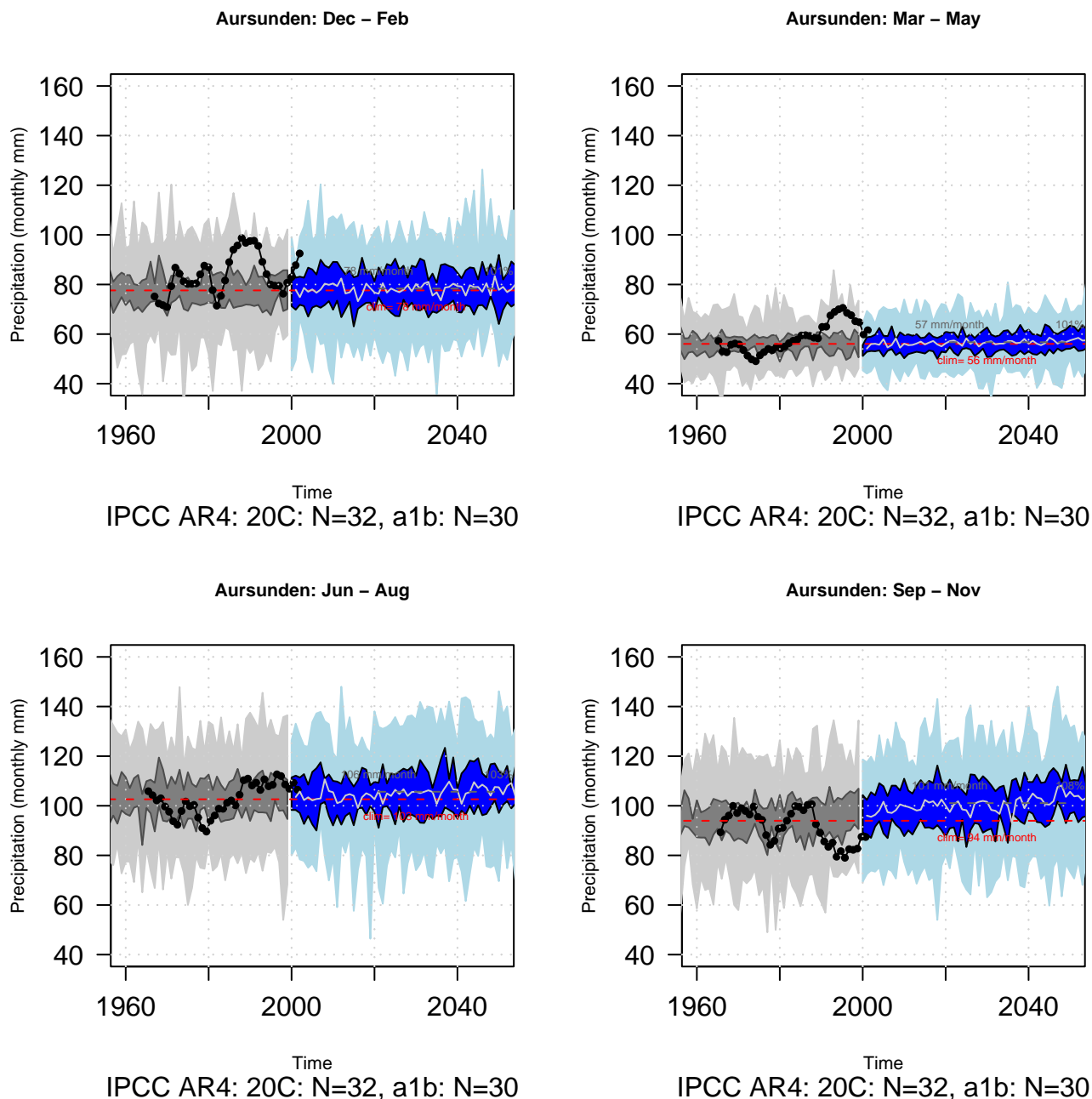


Figure 2.6 The figure shows the spread of empirically downscaled precipitation with precipitation as predictor from the 32 GCMs used for the historic period 1958 -2000 and the 30 GCMs for the future period 2000-2050 following the SRES A1b emission scenario. Projections are derived for four seasons; winter (upper left), spring (upper right), summer (lower left) and autumn (lower right). Mean temperature for the catchment as a whole, estimated from observations, is drawn as a dotted black curve.

2.7 Nybergsund

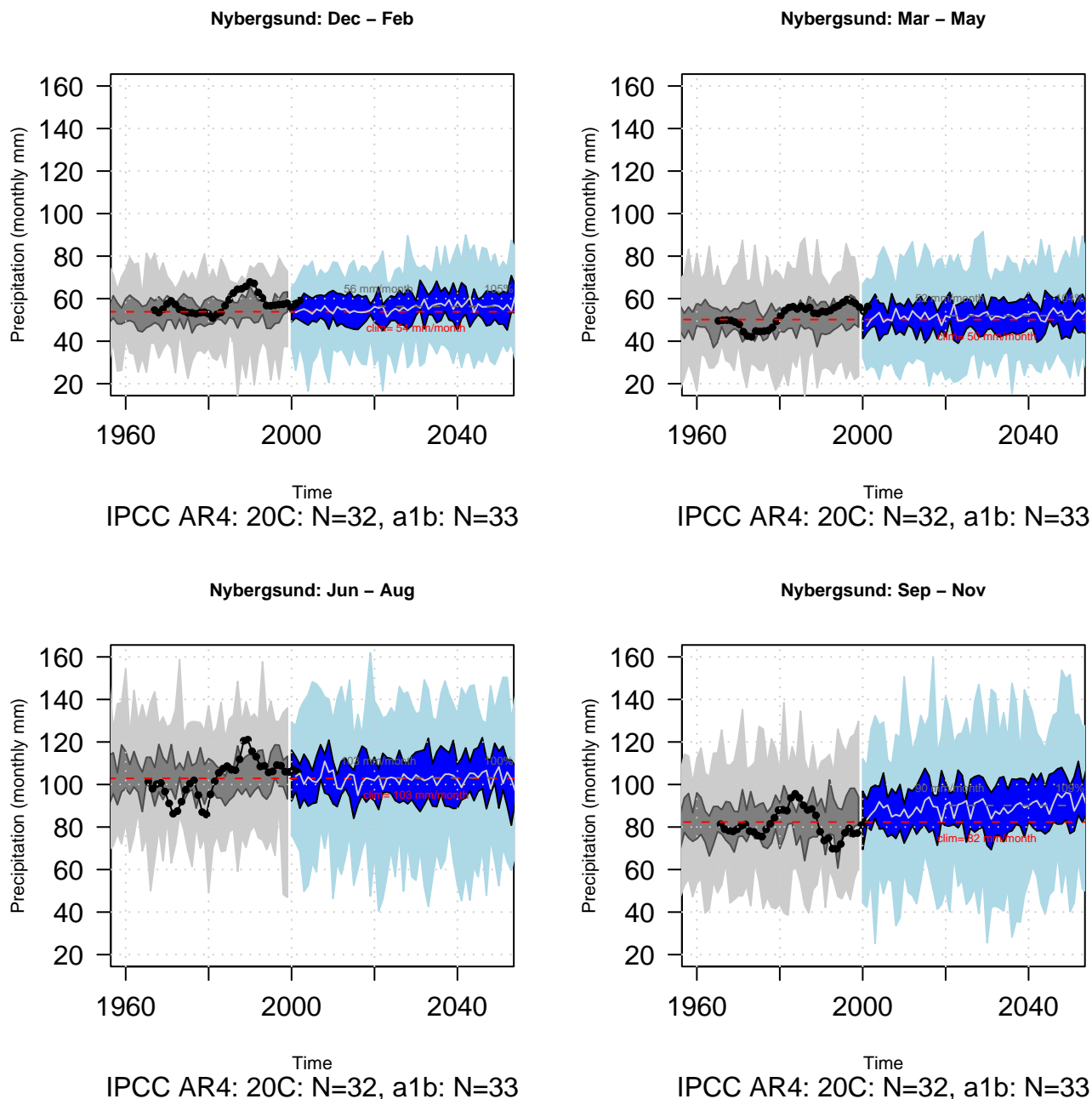


Figure 2.7 The figure shows the spread of empirically downscaled precipitation with precipitation as predictor from the 32 GCMs used for the historic period 1958 -2000 and the 33 GCMs for the future period 2000-2050 following the SRES A1b emission scenario. Projections are derived for four seasons; winter (upper left), spring (upper right), summer (lower left) and autumn (lower right). Mean temperature for the catchment as a whole, estimated from observations, is drawn as a dotted black curve.

2.8 Knappom

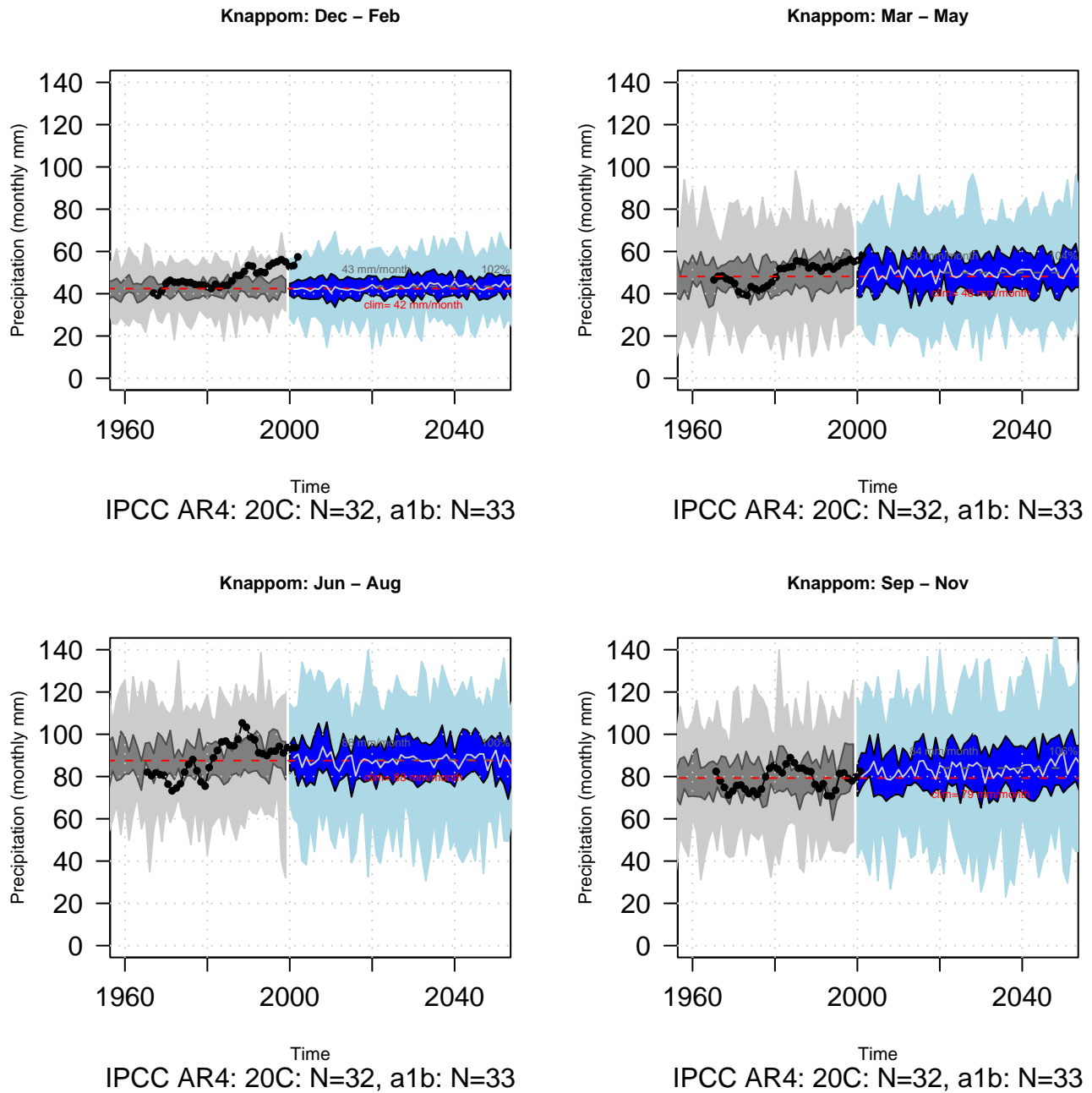


Figure 2.8 The figure shows the spread of empirically downscaled precipitation with precipitation as predictor from the 32 GCMs used for the historic period 1958 -2000 and the 33 GCMs for the future period 2000-2050 following the SRES A1b emission scenario. Projections are derived for four seasons; winter (upper left), spring (upper right), summer (lower left) and autumn (lower right). Mean temperature for the catchment as a whole, estimated from observations, is drawn as a dotted black curve.

2.9 Risefoss

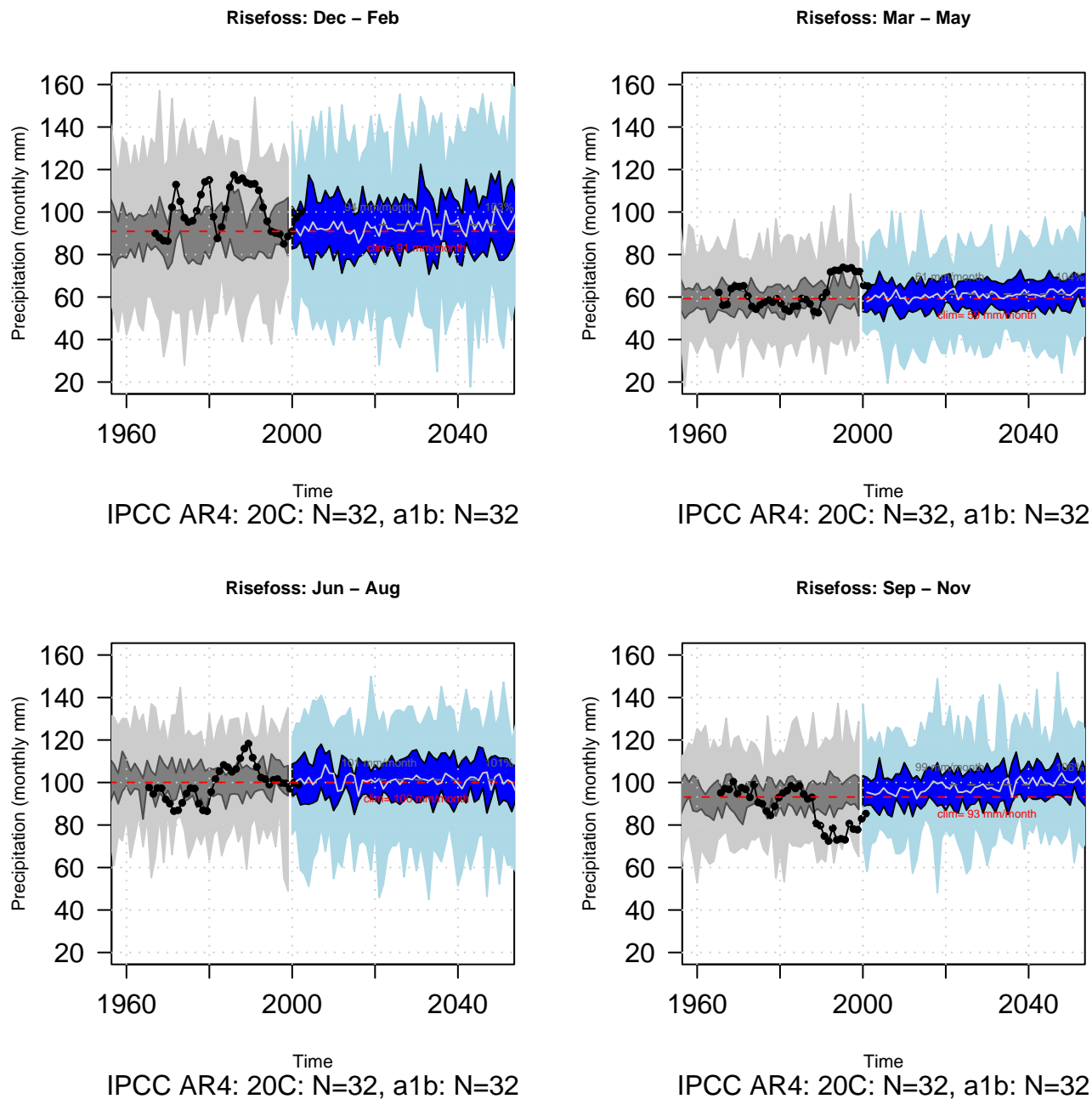


Figure 2.9 The figure shows the spread of empirically downscaled precipitation with precipitation as predictor from the 32 GCMs used for the historic period 1958 -2000 and the 32 GCMs for the future period 2000-2050 following the SRES A1b emission scenario. Projections are derived for four seasons; winter (upper left), spring (upper right), summer (lower left) and autumn (lower right). Mean temperature for the catchment as a whole, estimated from observations, is drawn as a dotted black curve.

2.10 Farstad

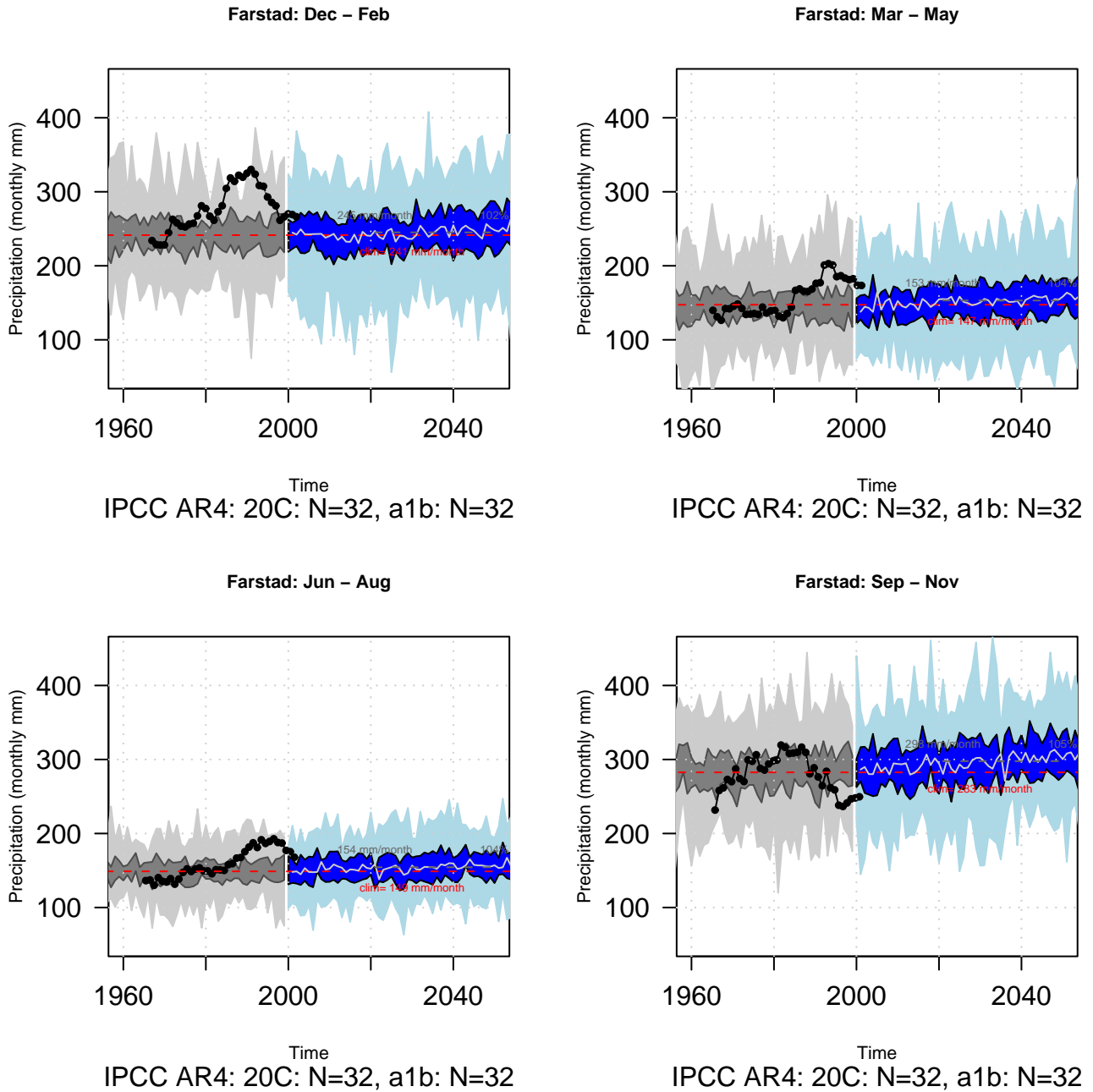


Figure 2.10 The figure shows the spread of empirically downscaled precipitation with precipitation as predictor from the 32 GCMs used for the historic period 1958 -2000 and the 32 GCMs for the future period 2000-2050 following the SRES A1b emission scenario. Projections are derived for four seasons; winter (upper left), spring (upper right), summer (lower left) and autumn (lower right). Mean temperature for the catchment as a whole, estimated from observations, is drawn as a dotted black curve.

2.11 Vistdal

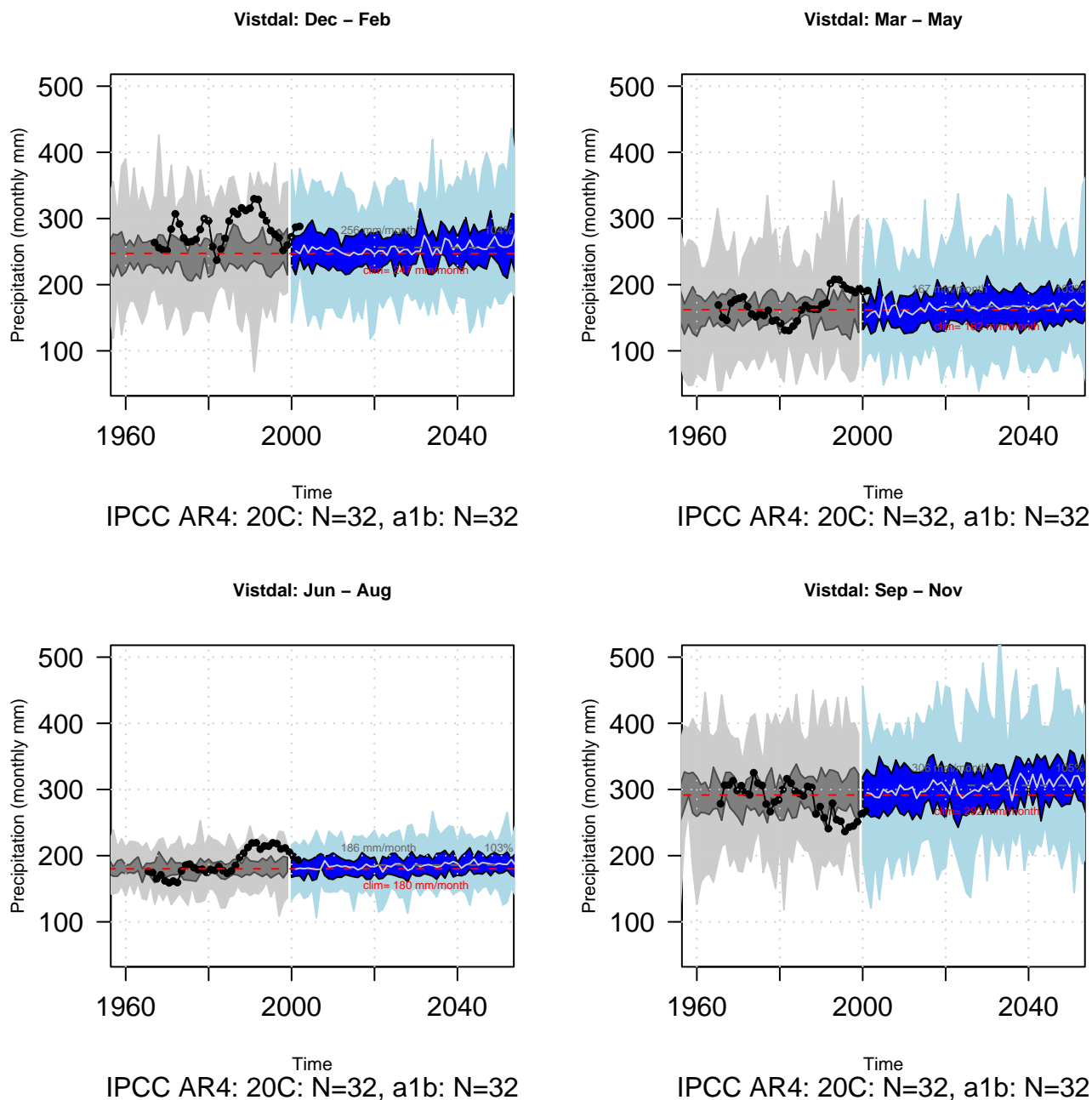


Figure 2.11 The figure shows the spread of empirically downscaled precipitation with precipitation as predictor from the 32 GCMs used for the historic period 1958 -2000 and the 32 GCMs for the future period 2000-2050 following the SRES A1b emission scenario. Projections are derived for four seasons; winter (upper left), spring (upper right), summer (lower left) and autumn (lower right). Mean temperature for the catchment as a whole, estimated from observations, is drawn as a dotted black curve.

2.12 Viksvatn

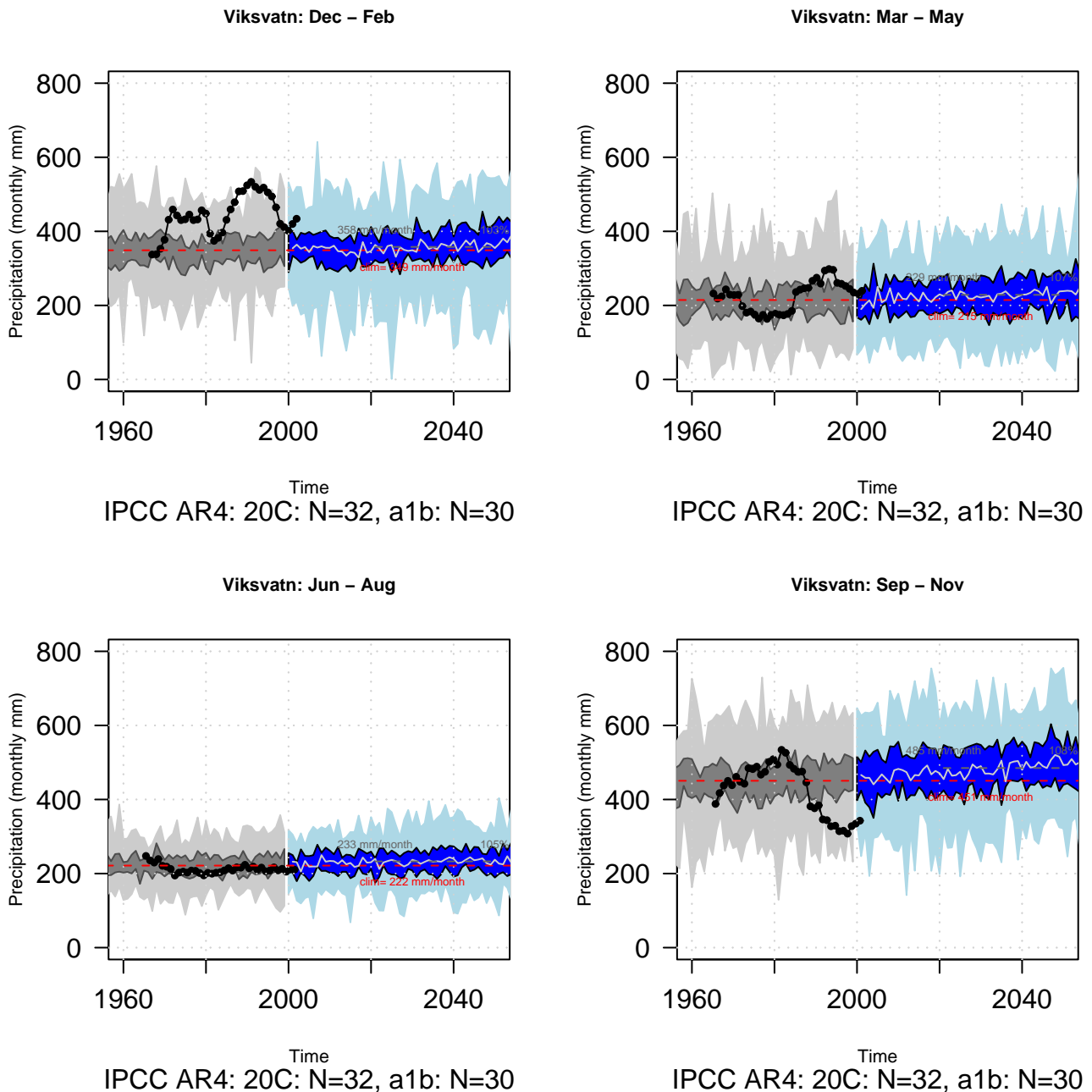


Figure 2.12 The figure shows the spread of empirically downscaled precipitation with precipitation as predictor from the 30 GCMs used for the historic period 1958 -2000 and the 32 GCMs for the future period 2000-2050 following the SRES A1b emission scenario. Projections are derived for four seasons; winter (upper left), spring (upper right), summer (lower left) and autumn (lower right). Mean temperature for the catchment as a whole, estimated from observations, is drawn as a dotted black curve.

2.13 Sjudalsvatn

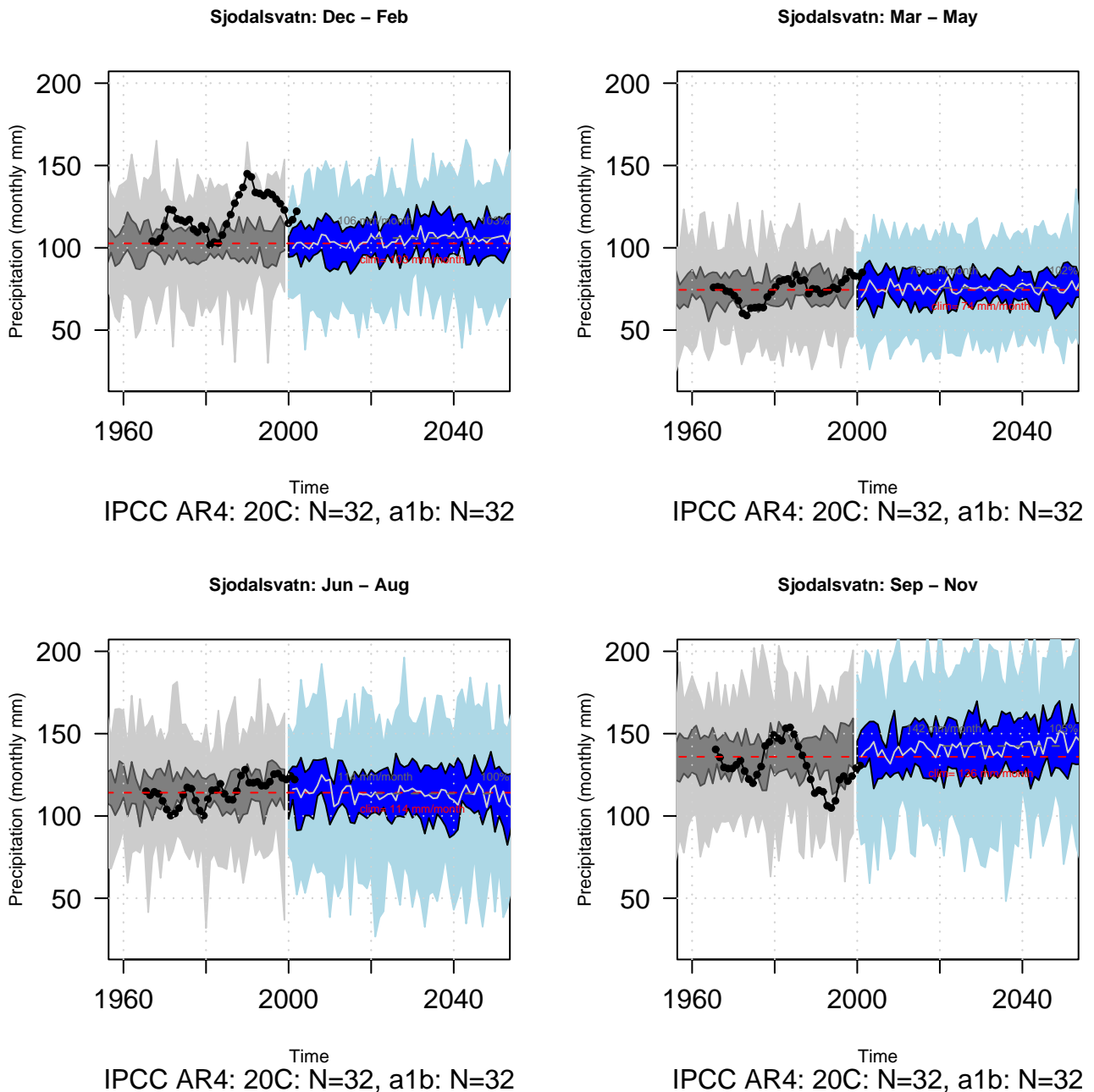


Figure 2.13 The figure shows the spread of empirically downscaled precipitation with precipitation as predictor from the 32 GCMs used for the historic period 1958 -2000 and the 32 GCMs for the future period 2000-2050 following the SRES A1b emission scenario. Projections are derived for four seasons; winter (upper left), spring (upper right), summer (lower left) and autumn (lower right). Mean temperature for the catchment as a whole, estimated from observations, is drawn as a dotted black curve.

2.14 Orsjøen

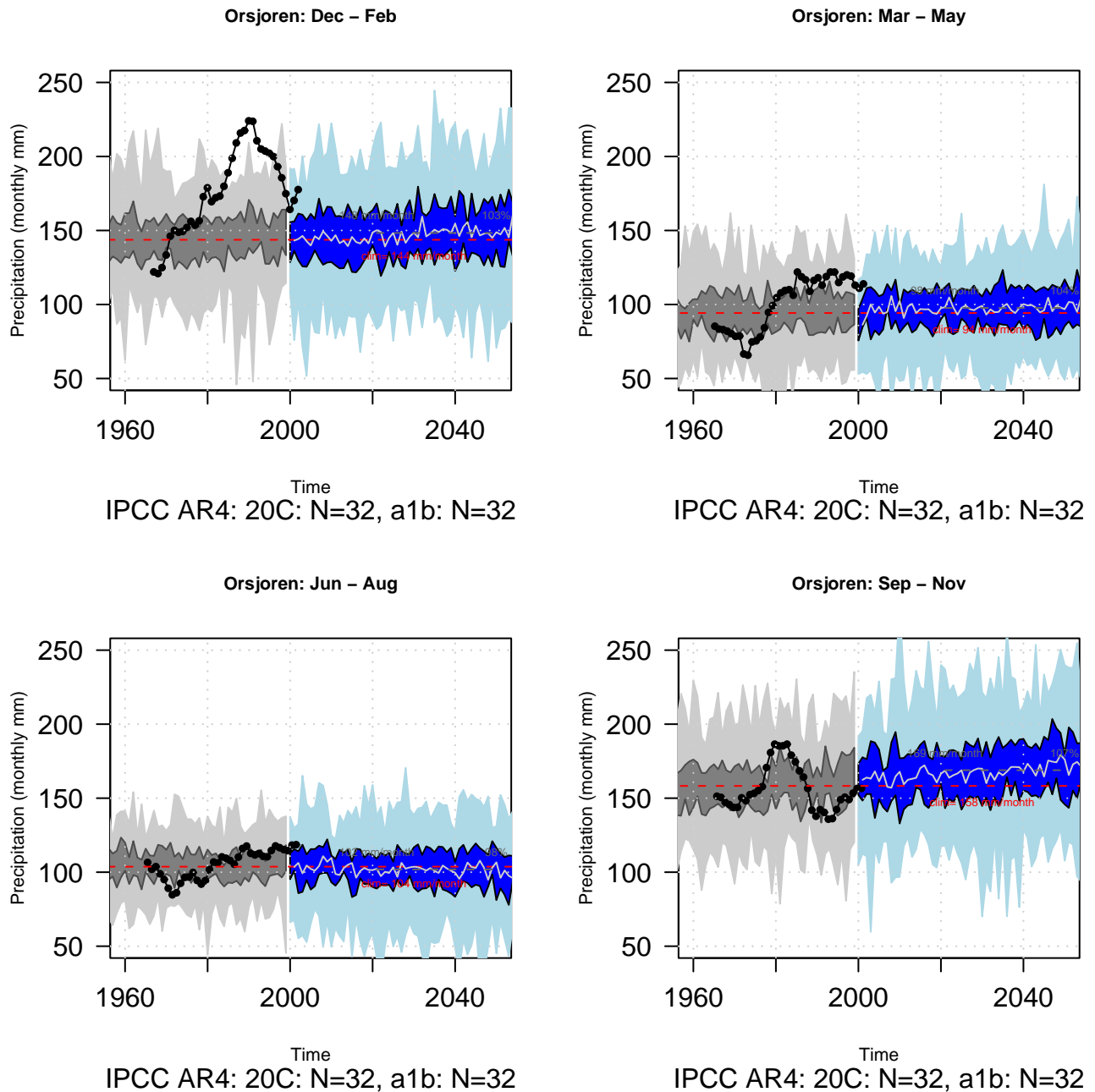


Figure 2.14 The figure shows the spread of empirically downscaled precipitation with precipitation as predictor from the 32 GCMs used for the historic period 1958 -2000 and the 32 GCMs for the future period 2000-2050 following the SRES A1b emission scenario. Projections are derived for four seasons; winter (upper left), spring (upper right), summer (lower left) and autumn (lower right). Mean temperature for the catchment as a whole, estimated from observations, is drawn as a dotted black curve.

2.15 Møsvatn

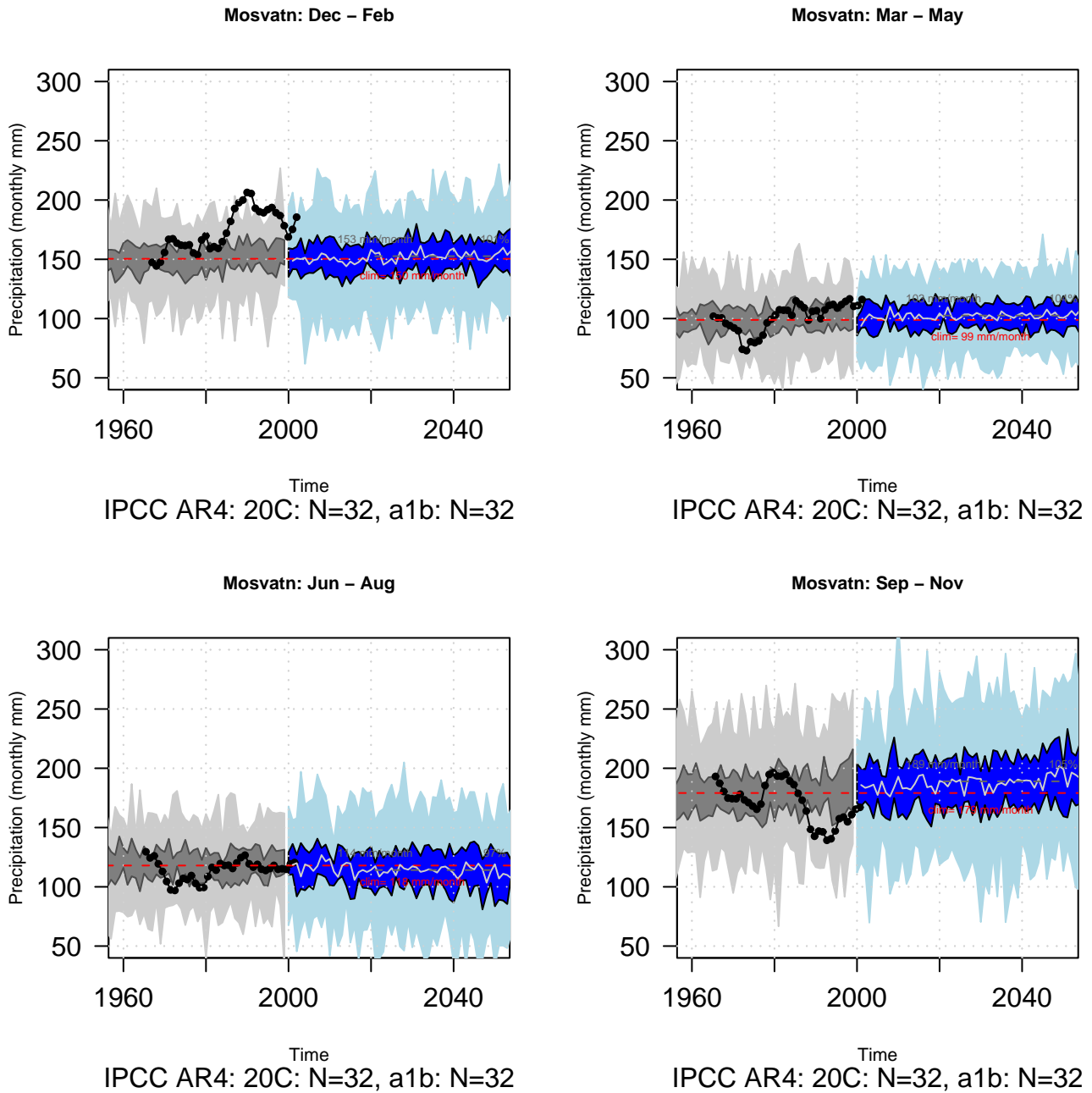


Figure 2.15 The figure shows the spread of empirically downscaled precipitation with precipitation as predictor from the 32 GCMs used for the historic period 1958 -2000 and the 32 GCMs for the future period 2000-2050 following the SRES A1b emission scenario. Projections are derived for four seasons; winter (upper left), spring (upper right), summer (lower left) and autumn (lower right). Mean temperature for the catchment as a whole, estimated from observations, is drawn as a dotted black curve.

2.16 Hølen

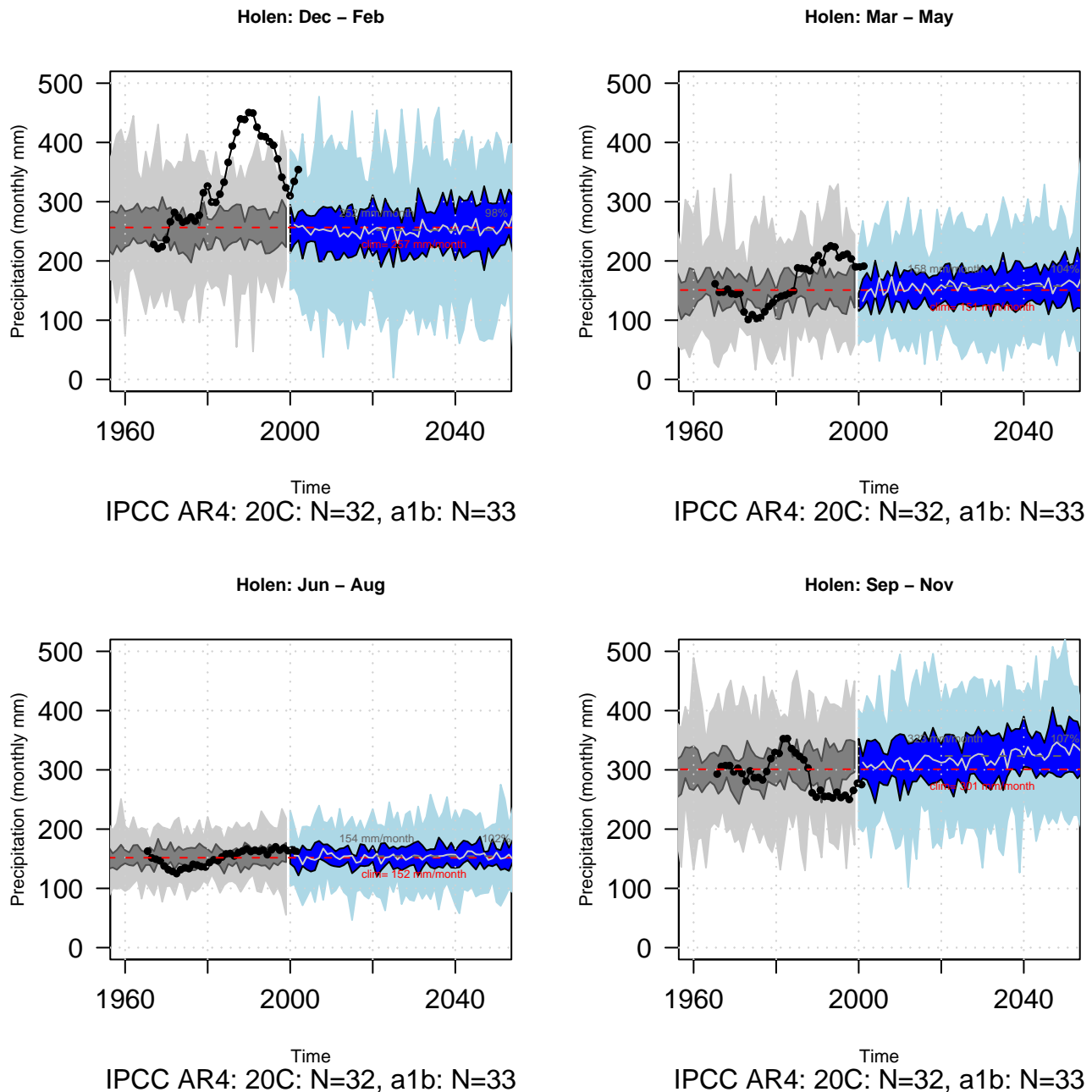


Figure 2.16 The figure shows the spread of empirically downscaled precipitation with precipitation as predictor from the 32 GCMs used for the historic period 1958 -2000 and the 33 GCMs for the future period 2000-2050 following the SRES A1b emission scenario. Projections are derived for four seasons; winter (upper left), spring (upper right), summer (lower left) and autumn (lower right). Mean temperature for the catchment as a whole, estimated from observations, is drawn as a dotted black curve.

2.17 Reinsnosvatn

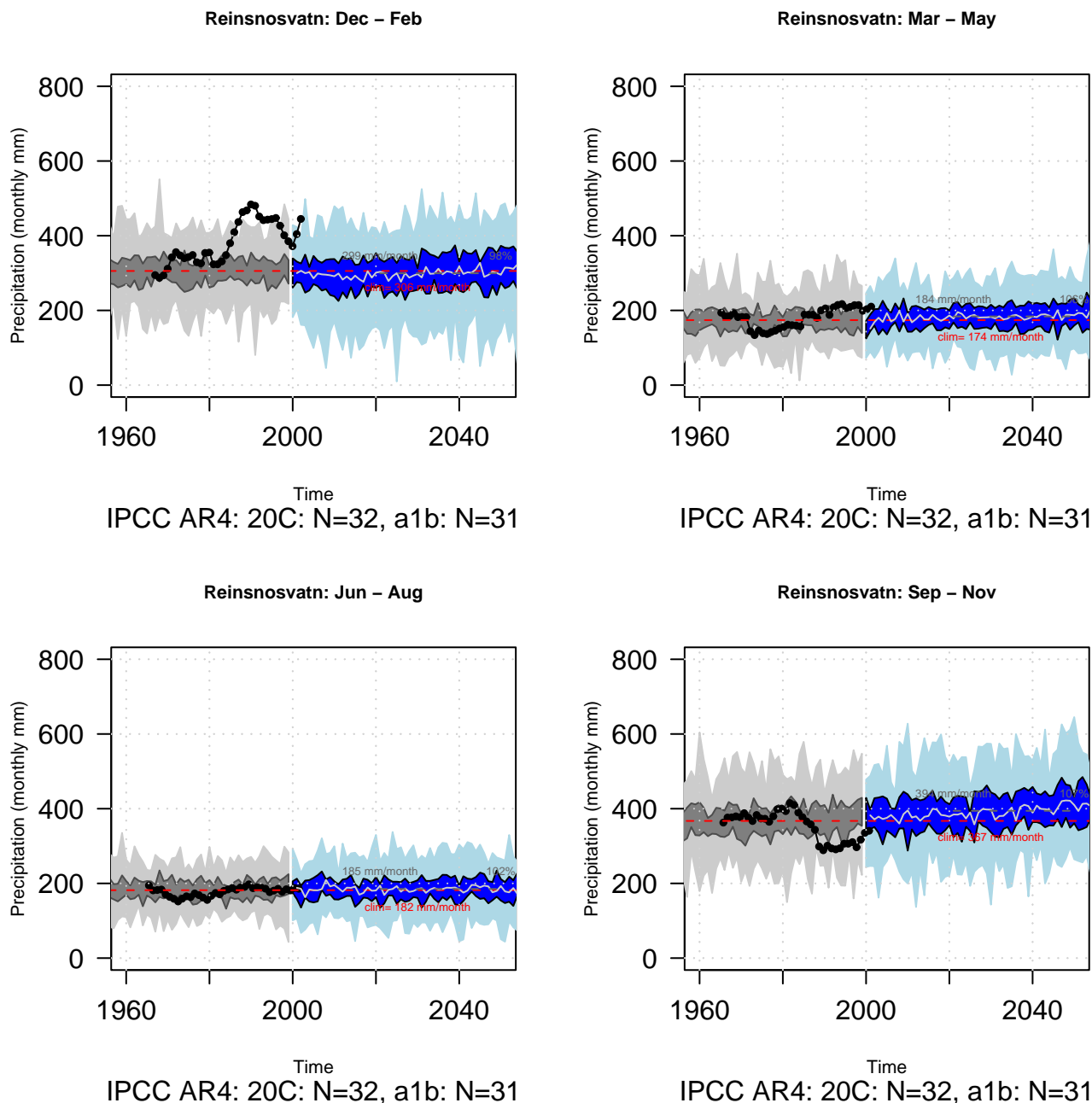


Figure 2.17 The figure shows the spread of empirically downscaled precipitation with precipitation as predictor from the 32 GCMs used for the historic period 1958 -2000 and the 31 GCMs for the future period 2000-2050 following the SRES A1b emission scenario. Projections are derived for four seasons; winter (upper left), spring (upper right), summer (lower left) and autumn (lower right). Mean temperature for the catchment as a whole, estimated from observations, is drawn as a dotted black curve.

2.18 Stordalsvatn

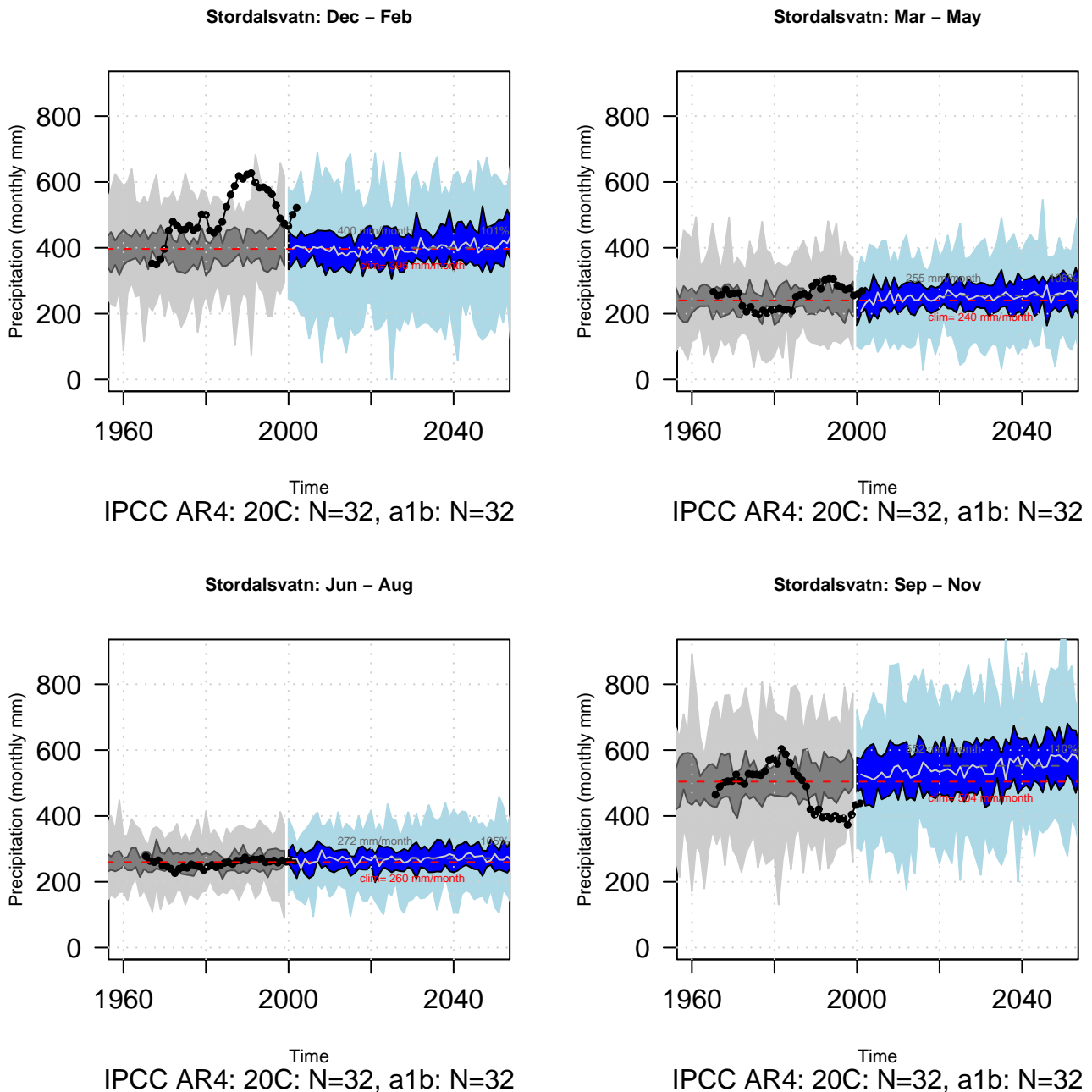


Figure 2.18 The figure shows the spread of empirically downscaled precipitation with precipitation as predictor from the 32 GCMs used for the historic period 1958 -2000 and the 32 GCMs for the future period 2000-2050 following the SRES A1b emission scenario. Projections are derived for four seasons; winter (upper left), spring (upper right), summer (lower left) and autumn (lower right). Mean temperature for the catchment as a whole, estimated from observations, is drawn as a dotted black curve.

2.19 Gjerstad

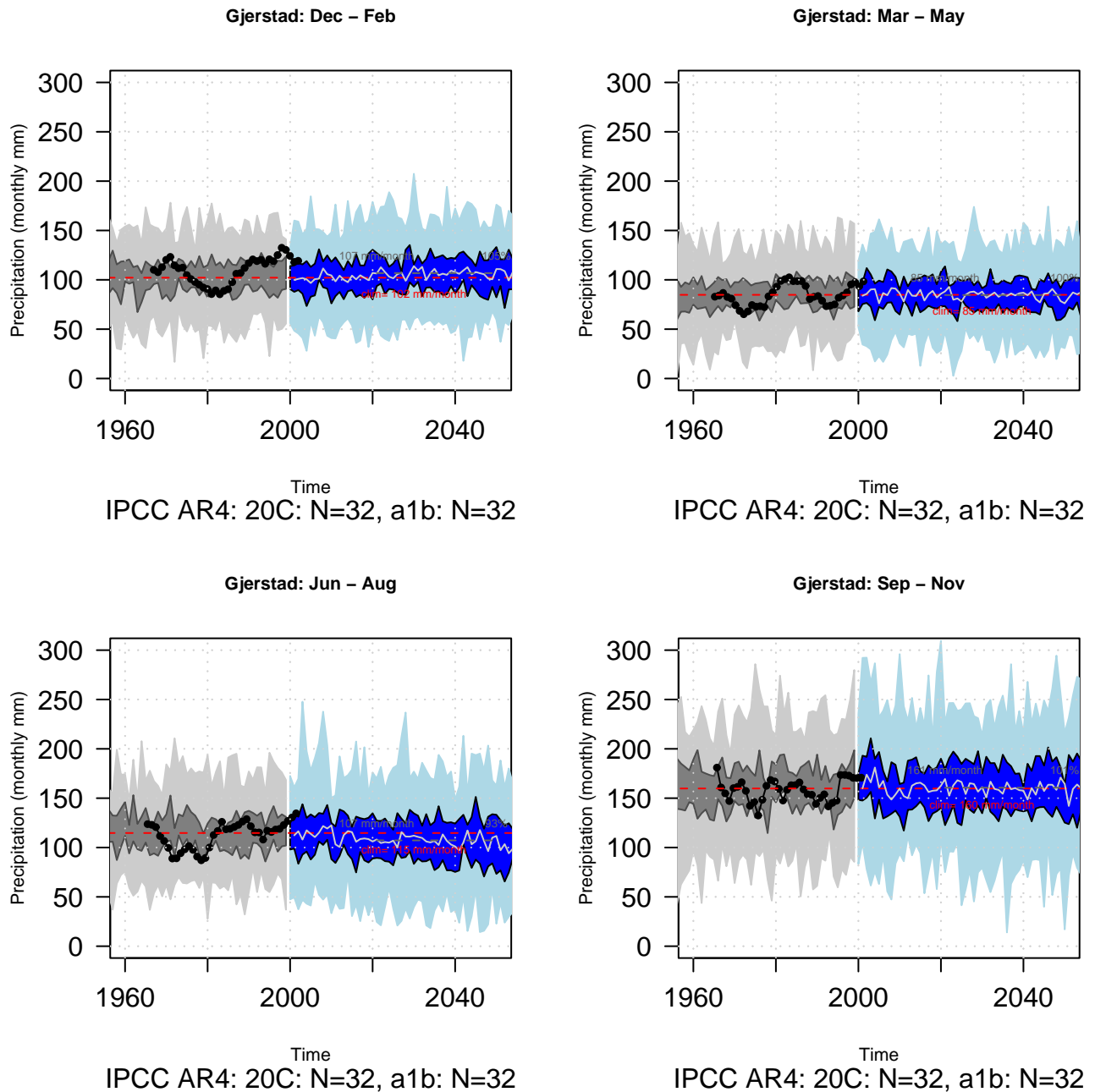


Figure 2.19 The figure shows the spread of empirically downscaled precipitation with precipitation as predictor from the 32 GCMs used for the historic period 1958 -2000 and the 32 GCMs for the future period 2000-2050 following the SRES A1b emission scenario. Projections are derived for four seasons; winter (upper left), spring (upper right), summer (lower left) and autumn (lower right). Mean temperature for the catchment as a whole, estimated from observations, is drawn as a dotted black curve.

2.20 Austenå

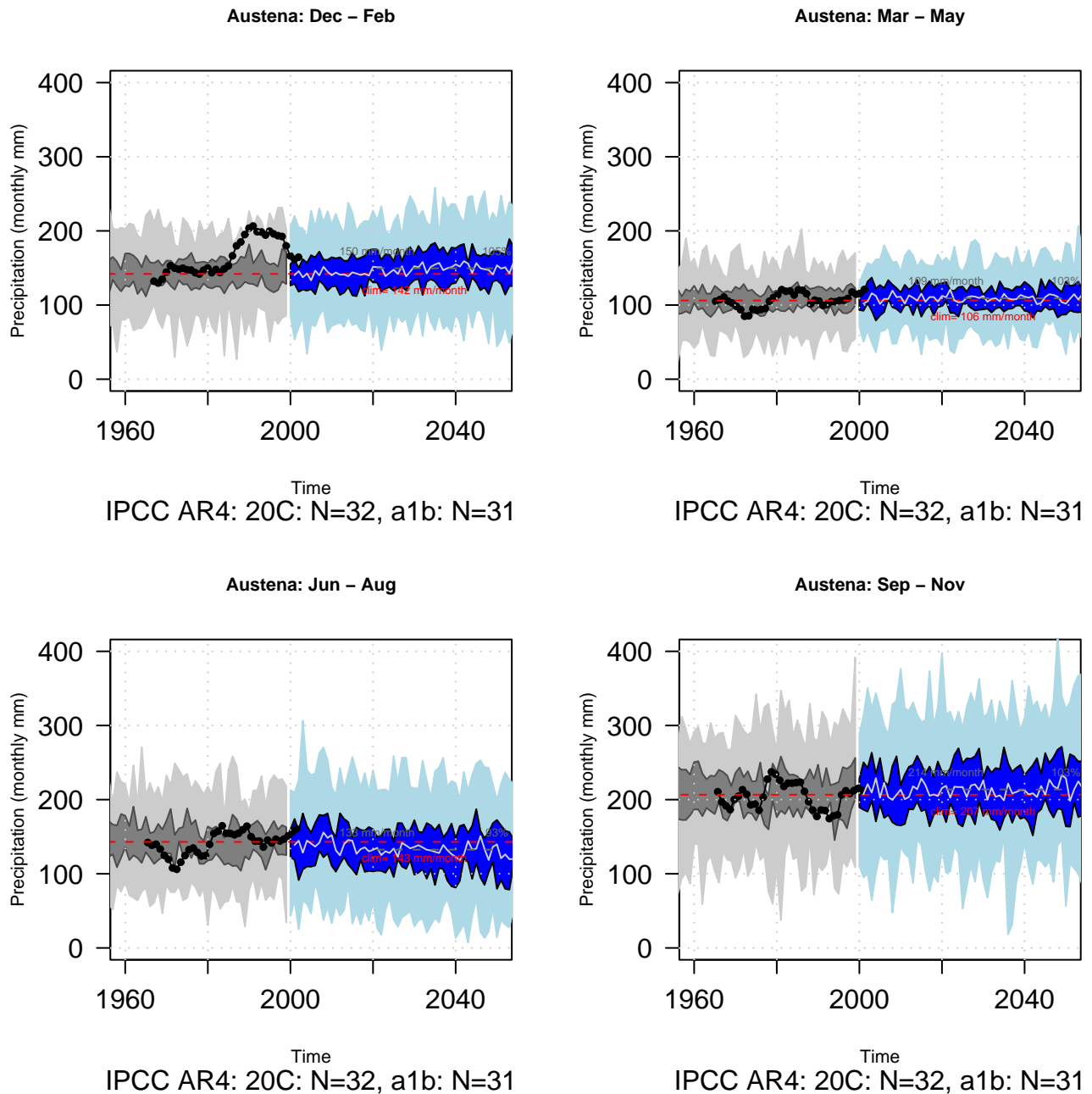


Figure 2.20 The figure shows the spread of empirically downscaled precipitation with precipitation as predictor from the 31 GCMs used for the historic period 1958 -2000 and the 32 GCMs for the future period 2000-2050 following the SRES A1b emission scenario. Projections are derived for four seasons; winter (upper left), spring (upper right), summer (lower left) and autumn (lower right). Mean temperature for the catchment as a whole, estimated from observations, is drawn as a dotted black curve.

2.21 Flaksvatn

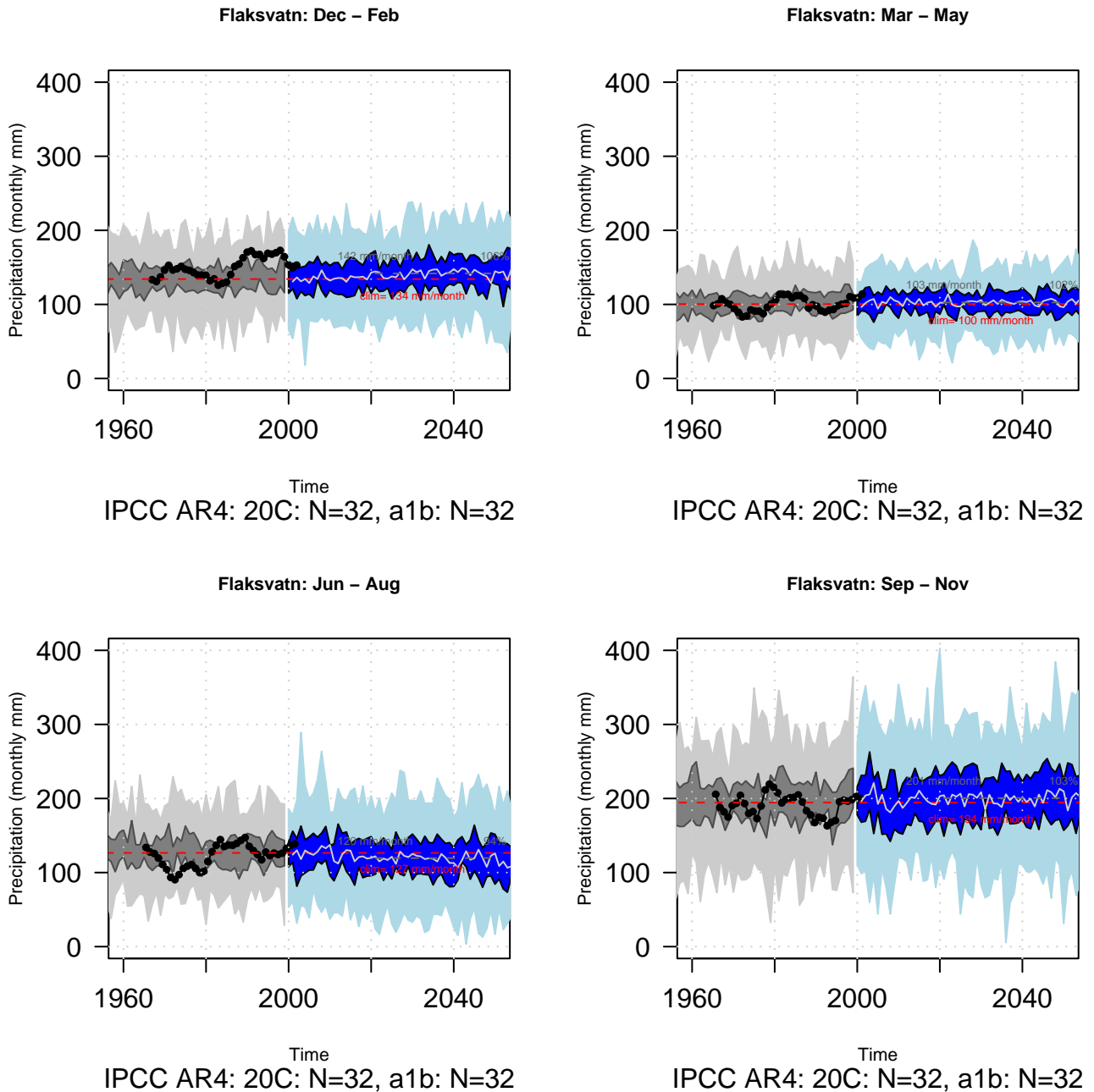


Figure 2.21 The figure shows the spread of empirically downscaled precipitation with precipitation as predictor from the 32 GCMs used for the historic period 1958 -2000 and the 32 GCMs for the future period 2000-2050 following the SRES A1b emission scenario. Projections are derived for four seasons; winter (upper left), spring (upper right), summer (lower left) and autumn (lower right). Mean temperature for the catchment as a whole, estimated from observations, is drawn as a dotted black curve.

2.22 Sandvatn

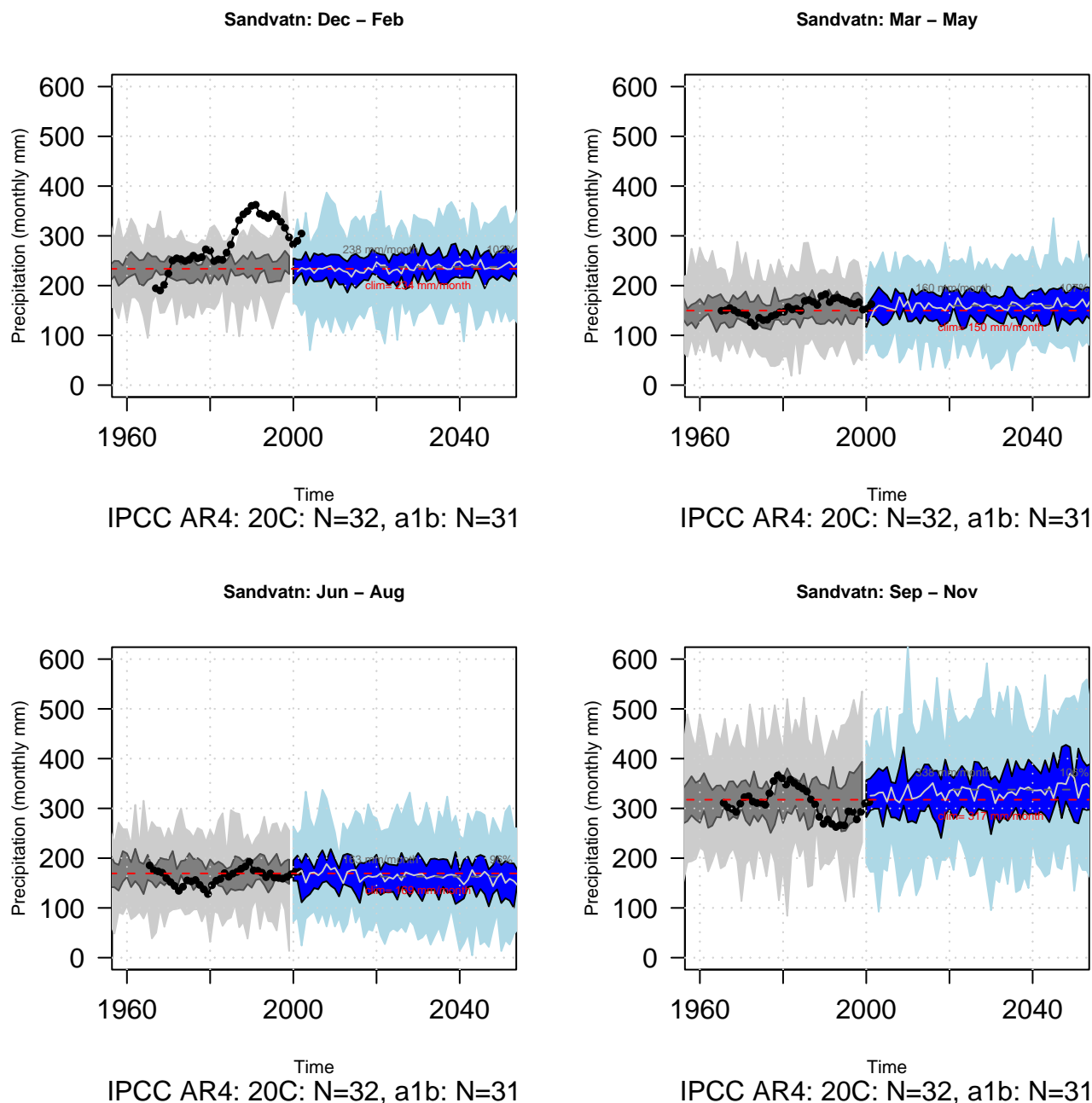


Figure 2.22 The figure shows the spread of empirically downscaled precipitation with precipitation as predictor from the 31 GCMs used for the historic period 1958 -2000 and the 32 GCMs for the future period 2000-2050 following the SRES A1b emission scenario. Projections are derived for four seasons; winter (upper left), spring (upper right), summer (lower left) and autumn (lower right). Mean temperature for the catchment as a whole, estimated from observations, is drawn as a dotted black curve.

2.23 Årdal

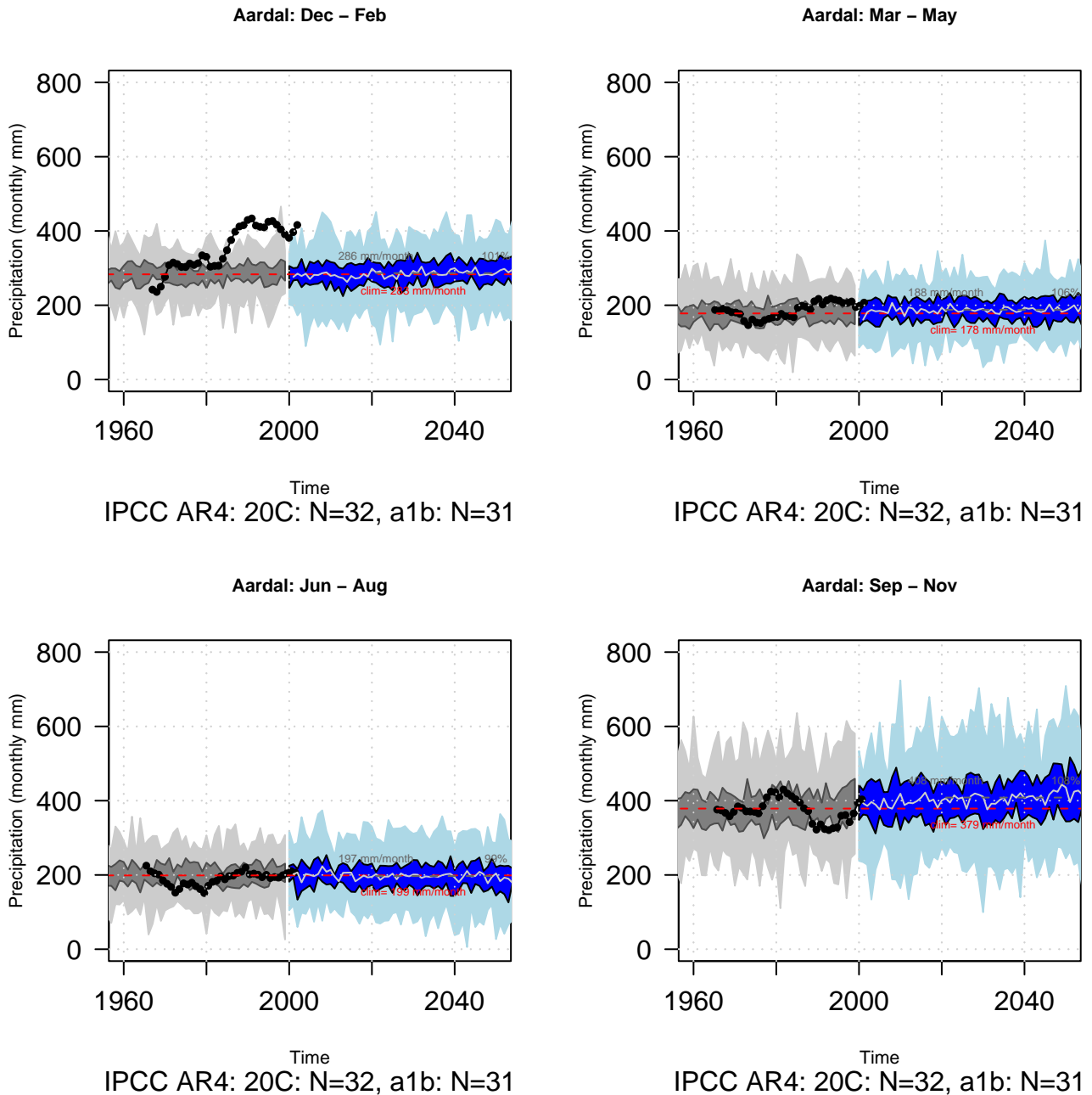


Figure 2.23 The figure shows the spread of empirically downscaled precipitation with precipitation as predictor from the 32 GCMs used for the historic period 1958 -2000 and the 31 GCMs for the future period 2000-2050 following the SRES A1b emission scenario. Projections are derived for four seasons; winter (upper left), spring (upper right), summer (lower left) and autumn (lower right). Mean temperature for the catchment as a whole, estimated from observations, is drawn as a dotted black curve..

2.24 Hetland

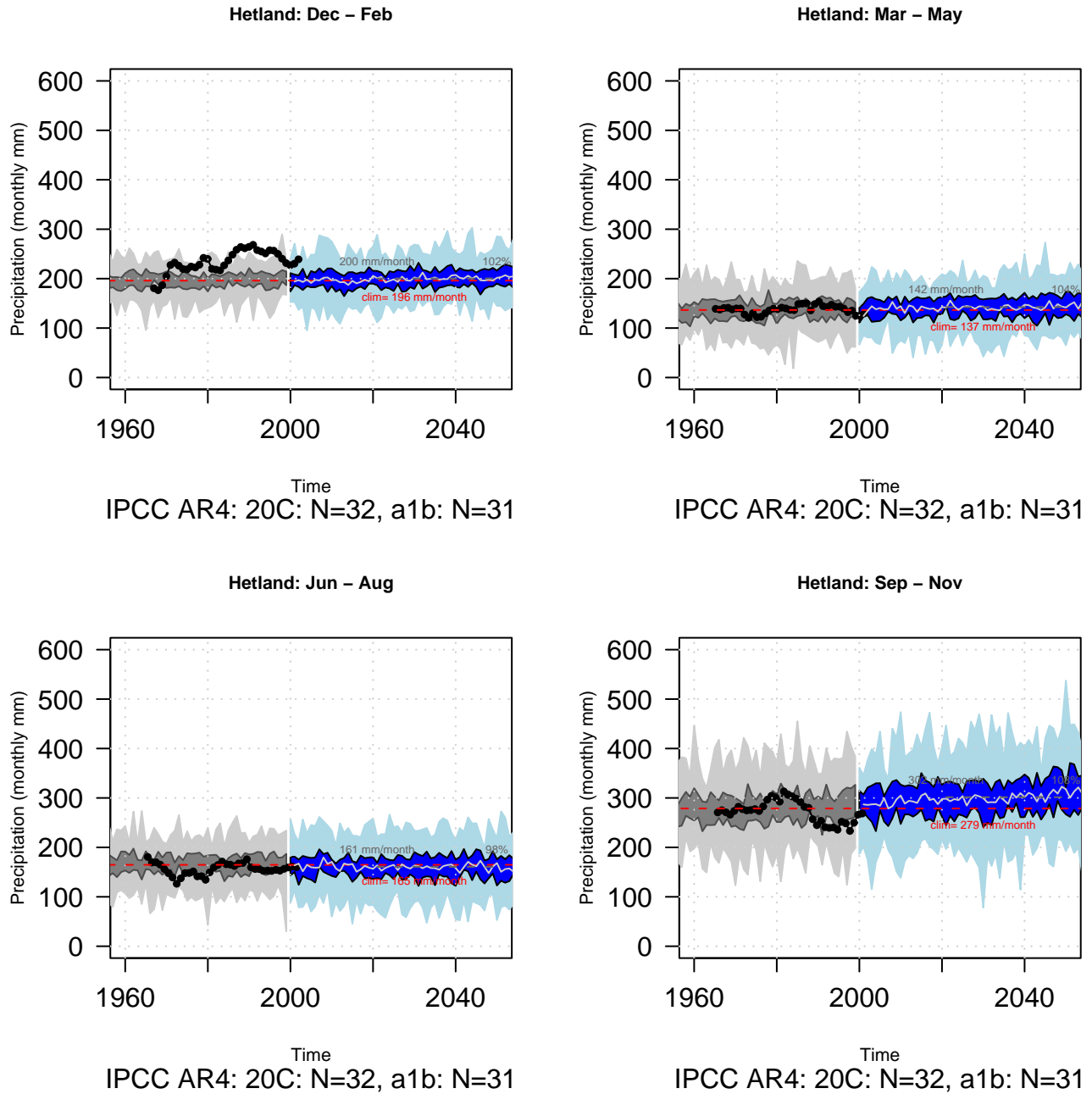


Figure 2.24 The figure shows the spread of empirically downscaled precipitation with precipitation as predictor from the 32 GCMs used for the historic period 1958 -2000 and the 31 GCMs for the future period 2000-2050 following the SRES A1b emission scenario. Projections are derived for four seasons; winter (upper left), spring (upper right), summer (lower left) and autumn (lower right). Mean temperature for the catchment as a whole, estimated from observations, is drawn as a dotted black curve.

2.25 Lyse

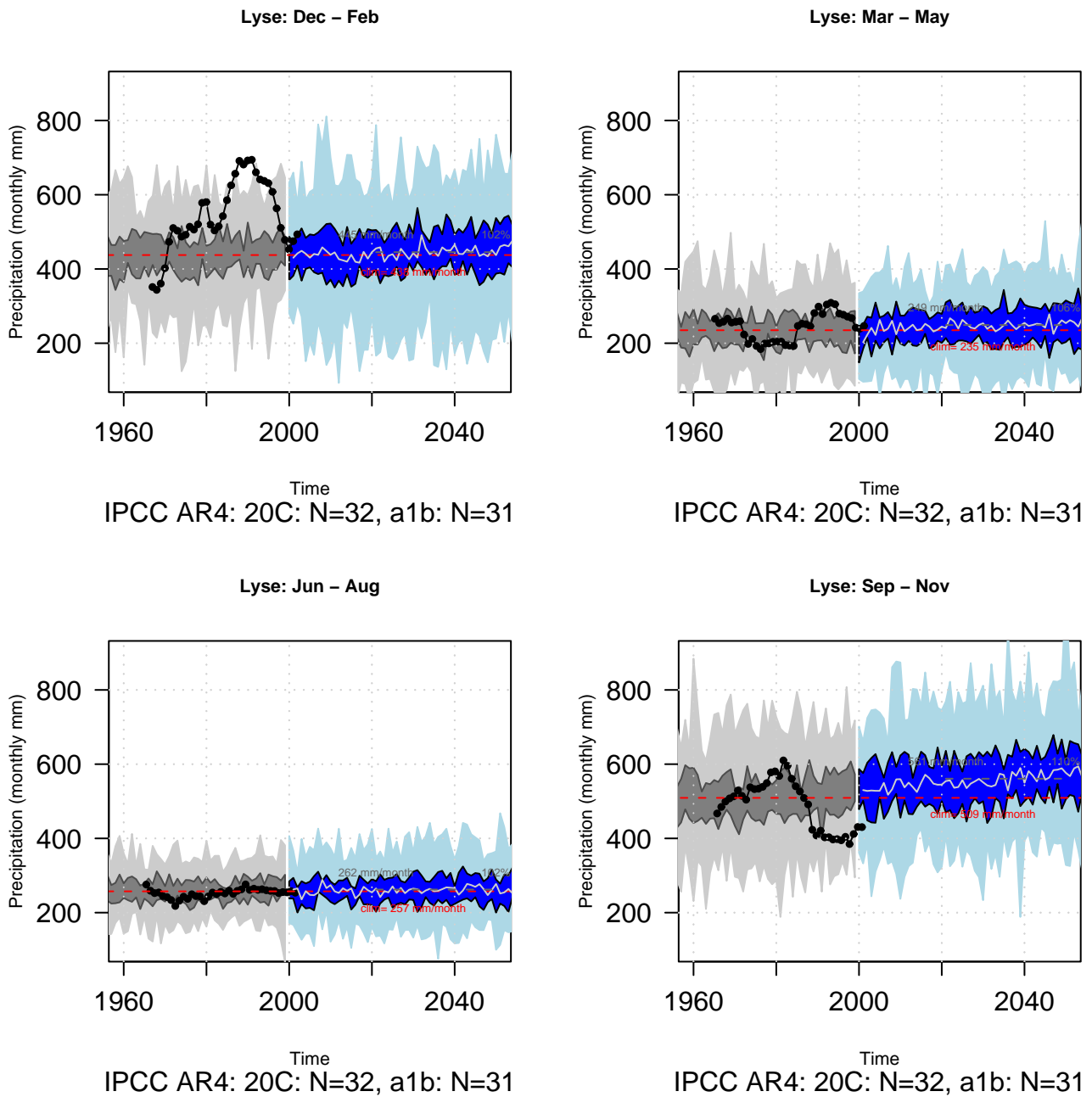


Figure 2.25 The figure shows the spread of empirically downscaled precipitation with precipitation as predictor from the 32 GCMs used for the historic period 1958 -2000 and the 31 GCMs for the future period 2000-2050 following the SRES A1b emission scenario. Projections are derived for four seasons; winter (upper left), spring (upper right), summer (lower left) and autumn (lower right). Mean temperature for the catchment as a whole, estimated from observations, is drawn as a dotted black curve.

3 Projections of precipitation for twenty-five Norwegian catchments; results from the Norwegian RegClim project

The long-term trends are more reliable than the decadal variations, and it is important to focus the early part of these long term trends. Thus, it is expected that the statistics of the precipitation for the future will be shifted slightly with respect to the present climate – towards the values corresponding to a climate scenario consistent with a stronger anthropogenic global warming.

3.1 Masi

Masi is situated in Northern Norway (Fig. 2.1 in Engen-Skaugen et al, 2008a). The size of the catchment is ~5600 km² (Table 2.1 in Engen-Skaugen et al, 2008a). The catchment rang from ~1090 to ~270 m a. s. l. (Fig. 2.2 in Engen-Skaugen et al, 2008a). Annual precipitation in the region is ~450 mm (Table 2.1 in Engen-Skaugen et al, 2008a). Most of the precipitation falls in summer (Fig. 3.18 in Engen-Skaugen et al, 2008a). In the Norwegian project Regional Climate development under global warming (RegClim <http://regclim.met.no>), annual increase in precipitation for the time period 2071-2100 compared to the time period 1961-1990 is projected to ~5-15% in the area. The largest increase is expected in the autumn (~15-25 %). No change in precipitation is projected during summer (~-5 - 5%) (Iversen et al., 2005). The estimates are based on dynamically downscaling of two global climate model runs following the emission scenario B2. The projections for the period 2020-2050 compared to 1980-1999 following the ECHAM4 GSDIO model and IS92a emission scenario, show similar results for precipitation; a increase in autumn (~15-20 %), no change in winter (~-5 - -5 %) and spring (~-5 - -5 %), and increased precipitation in summer (~10 - 15 %) (Førland et al., 2000; Bjørge et al., 2000).

3.2 Kobbvatn

Kobbvatn is situated in northern Norway (Fig. 2.1 in Engen-Skaugen et al, 2008a). The catchment size is ~390 km² (Table 2.1 in Engen-Skaugen et al, 2008a), it drains towards southwest. The catchments altitude rang from ~1520 to ~ 8 m a. s. l. (Fig. 2.2 in Engen-Skaugen et al, 2008a). Annual precipitation in the region is ~2550 mm (Table 2.1 in Engen-Skaugen et al, 2008a). The precipitation is spread through out the year, the largest rainfall comes from September until March (Fig. 3.10 in Engen-Skaugen et al, 2008a). In the Norwegian project Regional Climate development under global warming (RegClim <http://regclim.met.no>), annual increase in precipitation for the time period 2071-2100 compared to the time period 1961-1990 is projected to ~5-15% in the area. The largest increase is expected in the autumn (~20 - 25 %). Increase in precipitation is projected in spring (~10-15%), minor changes in winter (~-5-5%) and summer (~0-5%) (Iversen et al., 2005). The estimates are based on dynamically downscaling of two global climate model runs following the emission scenario B2. The projections for the period 2020-2050 compared to 1980-1999 following the ECHAM4 GSDIO model and IS92a emission scenario, show similar results for precipitation; a increase in autumn (~5 - 10 %), minor changes in other seasons (~ 0 - 5 %) (Førland et al., 2000; Bjørge et al., 2000). Increase in summer precipitation as for the combined B2 projection is not found in the IS92a projection.

3.3 Nervoll

Nervoll is situated in northern Norway (Fig. 2.1 in Engen-Skaugen et al, 2008a). The catchment size is ~650 km² (Table 2.1 in Engen-Skaugen et al, 2008a), it drains northwards. It is a high mountain catchment ranging from ~1700 to ~ 360 m a. s. l. (Fig. 2.2 in Engen-Skaugen et al, 2008a). Annual precipitation in the region is ~1550 mm (Table 2.1 in Engen-Skaugen et al, 2008a). The precipitation is spread through out the year, the largest rainfall comes from July until March (Fig. 3.9 in Engen-Skaugen et al, 2008a). In the Norwegian project Regional Climate development under global warming (RegClim <http://regclim.met.no>), annual increase in precipitation for the time period 2071-2100 compared to the time period 1961-1990 is projected to ~5-15% in the area. The largest increase is expected in the autumn (~10-15 %). Increased

precipitation is projected in winter and spring are projected (~5 – 10 %), less increase in summer (~0 – 5 %) (Iversen et al., 2005). The estimates are based on dynamically downscaling of two global climate model runs following the emission scenario B2. The projections for the period 2020-2050 compared to 1980-1999 following the ECHAM4 GSDIO model and IS92a emission scenario, show similar results for precipitation; increased precipitation in autumn (~15-20 %), minor changes in winter and spring. Increased precipitation in summer (~5 – 10 %) differs from the combined B2 projection (Førland et al., 2000; Bjørge et al., 2000). Increased precipitation in winter and spring as for the combined B2 projection is not found in the IS92a projection.

3.4 Kjelstad

Kjelstad is situated in the middle of Norway on the eastern side (Fig. 2.1 in Engen-Skaugen et al, 2008a). It is a small catchment ~142 km² (Table 2.1 in Engen-Skaugen et al, 2008a), it drains towards northwest. It is a high mountain catchment ranging from ~1170 to ~ 280 m a. s. l. (Fig. 2.3). Annual precipitation in the region is ~1450 mm (Table 2.1 in Engen-Skaugen et al, 2008a). The precipitation is fairly spread through out the year with a peak in autumn (Fig. 3.8 in Engen-Skaugen et al, 2008a). In the Norwegian project Regional Climate development under global warming (RegClim <http://regclim.met.no>), annual increase in precipitation for the time period 2071-2100 compared to the time period 1961-1990 is projected to ~5-15% in the area. The largest increase is expected in the autumn (~20-25 %), but also in winter (~10 - 15 %) and spring (~10 - 15 %). Decrease in precipitation is projected during summer (~-5 – 0 %) (Iversen et al., 2005). The estimates are based on dynamically downscaling of two global climate model runs following the emission scenario B2. The projections for the period 2020-2050 compared to 1980-1999 following the ECHAM4 GSDIO model and IS92a emission scenario, show similar results for precipitation; increased precipitation in autumn (~10-15 %) and winter (~ 5 - 10%). The opposite is found in spring and summer though; minor decrease in spring (~-5 - 0%) and increase in summer (~10 - 15%) (Førland et al., 2000; Bjørge et al., 2000).

3.5 Rathe

Rathe is situated in the middle of Norway on the eastern side (Fig. 2.1 in Engen-Skaugen et al, 2008a). It is a large catchment ~3050 km² (Table 2.1 in Engen-Skaugen et al, 2008a), it drains towards northwest. It is a high mountain catchment ranging from ~1762 to ~ 44 m a. s. l. (Fig. 2.3 in Engen-Skaugen et al, 2008a). Annual precipitation in the region is ~1300 mm (Table 2.1 in Engen-Skaugen et al, 2008a). The precipitation is fairly spread through out the year with a peak in autumn (Fig. 3.7 in Engen-Skaugen et al, 2008a). In the Norwegian project Regional Climate development under global warming (RegClim <http://regclim.met.no>), annual increase in precipitation for the time period 2071-2100 compared to the time period 1961-1990 is projected to ~5 - 15% in the area. The largest increase is expected in the autumn (~20-25 %). Increased precipitation in winter (~10-15 %) and spring (~10-15 %) is projected as well. A decrease in precipitation is projected during summer (~-5 - 0 %) (Iversen et al., 2005). The estimates are based on dynamically downscaling of two global climate model runs following the emission scenario B2. The projections for the period 2020-2050 compared to 1980-1999 following the ECHAM4 GSDIO model and IS92a emission scenario, show similar results for precipitation; increased precipitation in autumn (~10-15 %) and winter (~5 - 10 %). The opposite is found in spring and summer though; decrease in spring (~-10 - 0%) and increase in summer (~10 - 15%) (Førland et al., 2000; Bjørge et al., 2000).

3.6 Aursunden

Aursunden is situated in the eastern part of Norway near the Swedish boarder (Fig. 2.1 in Engen-Skaugen et al, 2008a). The size of the catchment is ~850 km² (Table 2.1 in Engen-Skaugen et al, 2008a) the catchment rang from ~1525 to ~700 m a. s. l. (Fig. 2.3 in Engen-Skaugen et al, 2008a). Annual precipitation in the region is ~1000 mm (Table 2.1 in Engen-Skaugen et al, 2008a). The precipitation is distributed fairly equal throughout the year (Fig. 3.21 in Engen-Skaugen et al, 2008a). In the Norwegian project Regional Climate development under global warming (RegClim <http://regclim.met.no>), annual increase in precipitation for the time period 2071-2100 compared to the time period 1961-1990 is projected to ~12% in the area. The largest increase is expected in the autumn (~20-25 %), increase in precipitation is

also projected for winter (~10 - 15%) and spring (~10 - 15%). Reduced precipitation is projected during summer (~-5 - 0%). (Iversen et al., 2005). The estimates are based on dynamically downscaling of two global climate model runs following the emission scenario B2. The projections for the period 2020-2050 compared to 1980-1999 following the ECHAM4 GSDIO model and IS92a emission scenario, show similar results for precipitation; increased precipitation in autumn (~5-15 %) and winter (~5 - 10%). The opposite is found in spring and summer though; decrease in spring (~-10 - -5%) and increase in summer (~5 - 10%) (Førland et al., 2000; Bjørge et al., 2000).

3.7 Nybergsund

Nybergsund is situated in the eastern part of Norway with parts of the catchment in Sweden (Fig. 2.1 in Engen-Skaugen et al, 2008a). The size of the catchment is ~4420 km² (Table 2.1 in Engen-Skaugen et al, 2008a) the catchment rang from ~1755 to ~355 m a. s. l. (Fig. 2.3 in Engen-Skaugen et al, 2008a). Annual precipitation in the region is ~850 mm (Table 2.1 in Engen-Skaugen et al, 2008a). Most of the precipitation falls in summer and autumn (Fig. 3.19 in Engen-Skaugen et al, 2008a). In the Norwegian project Regional Climate development under global warming (RegClim <http://regclim.met.no>), annual increase in precipitation for the time period 2071-2100 compared to the time period 1961-1990 is projected to ~5 - 15% in the area. The largest increase is expected in the autumn (~20-25 %). Increase in precipitation is also projected for winter (~15 - 25 %) and spring (~10 - 15%). Minor change in precipitation is projected in summer (~-5 - 0%). (Iversen et al., 2005). The estimates are based on dynamically downscaling of two global climate model runs following the emission scenario B2. The projections for the period 2020-2050 compared to 1980-1999 following the ECHAM4 GSDIO model and IS92a emission scenario, show similar results for precipitation; increased precipitation in autumn (~5 - 10 %) and winter (~10 - 15 %). The opposite is found in spring and summer though; decrease in spring (~-10 - -5%) and increase in summer (~5 - 10%) (Førland et al., 2000; Bjørge et al., 2000).

3.8 Knappom

Knappom is situated eastern Norway on the Swedish boarder (Fig. 2.1 in Engen-Skaugen et al, 2008a). The size of the catchment is ~1650 km² (Table 2.1 in Engen-Skaugen et al, 2008a) the catchment rang from ~800 to ~180 m a. s. l. (Fig. 2.3 in Engen-Skaugen et al, 2008a). Annual precipitation in the region is ~750 mm (Table 2.1 in Engen-Skaugen et al, 2008a). The precipitation is distributed fairly equal throughout the year (Fig. 3.22 in Engen-Skaugen et al, 2008a). In the Norwegian project Regional Climate development under global warming (RegClim <http://regclim.met.no>), annual increase in precipitation for the time period 2071-2100 compared to the time period 1961-1990 is projected to ~5-15% in the area. The largest increase is expected in the autumn (~15-20 %). Marked increase is also projected in winter(~15 - 20%) and spring (~10 - 15 %). Decrease in precipitation is projected during summer (~-15 - 0%) (Iversen et al., 2005). The estimates are based on dynamically downscaling of two global climate model runs following the emission scenario B2. The projections for the period 2020-2050 compared to 1980-1999 following the ECHAM4 GSDIO model and IS92a emission scenario, show similar results for precipitation; increased precipitation in autumn (~5 - 10 %) and winter (~15 - 20 %). The opposite is found in spring and summer though; decrease in spring (~-10 - 0%) and increase in summer (~5 - 10%) (Førland et al., 2000; Bjørge et al., 2000).

3.9 Risefoss

Risefoss is situated in the north-western part of Norway (Fig. 2.1 in Engen-Skaugen et al, 2008a). The size of the catchment is ~743 km² (Table 2.1 in Engen-Skaugen et al, 2008a), it drains northwards. It is a high mountain catchment ranging from ~2286 to ~ 580 m a. s. l. (Fig. 2.3 in Engen-Skaugen et al, 2008a). Annual precipitation in the region is ~1000 mm (Table 2.1 in Engen-Skaugen et al, 2008a). The precipitation is fairly spread through out the year with a dip in spring (Fig. 3.6 in Engen-Skaugen et al, 2008a). In the Norwegian project Regional Climate development under global warming (RegClim <http://regclim.met.no>), annual increase in precipitation for the time period 2071-2100 compared to the time period 1961-1990 is projected to ~5 - 15% in the area. The largest increase is expected in the autumn (~20-25 %). Increased precipitation is also projected in winter (~15 - 20 %) and spring (~10 - 15 %). Minor

decrease in precipitation is projected during summer (~-5 - 0%) (Iversen et al., 2005). The estimates are based on dynamically downscaling of two global climate model runs following the emission scenario B2. The projections for the period 2020-2050 compared to 1980-1999 following the ECHAM4 GSDIO model and IS92a emission scenario, show similar results for precipitation; increased precipitation in autumn (~5 - 15 %) and winter (~10 - 15 %). The opposite is found in spring and summer though; decrease in spring (~-5 - 0%) and increase in summer (~10 - 15%) (Førland et al., 2000; Bjørge et al., 2000).

3.10 Farstad

Farstad is situated in the coastal part of north-western Norway (Fig. 2.1 in Engen-Skaugen et al, 2008a). The size of the catchment is ~23 km² (Table 2.1 in Engen-Skaugen et al, 2008a) ranging from ~667 to ~19 m a. s. l. (Fig. 2.4 in Engen-Skaugen et al, 2008a). Annual precipitation in the region is ~2500 mm (Table 2.1 in Engen-Skaugen et al, 2008a). The precipitation is fairly spread through out the year with a dip in spring and summer (Fig. 3.5 in Engen-Skaugen et al, 2008a). In the Norwegian project Regional Climate development under global warming (RegClim <http://regclim.met.no>), annual increase in precipitation for the time period 2071-2100 compared to the time period 1961-1990 is projected to ~15 - 20% in the area. The largest increase is expected in the autumn (~20-25 %) Marked increase in precipitation is projected also for the other seasons (~15 - 20%). (Iversen et al., 2005). The estimates are based on dynamically downscaling of two global climate model runs following the emission scenario B2. The projections for the period 2020-2050 compared to 1980-1999 following the ECHAM4 GSDIO model and IS92a emission scenario, show similar results for precipitation; a increase in autumn (~25 - 30 %), winter (~5 - 10 %) and summer (~15-20 %). Reduced precipitation is projected in spring (~-10 - -5 %), though. (Førland et al., 2000; Bjørge et al., 2000).

3.11 Vistdal

Vistdal is situated near the coastal part of north-western Norway (Fig. 2.1 in Engen-Skaugen et al, 2008a). The size of the catchment is ~66 km² (Table 2.1 in Engen-Skaugen et al, 2008a) the catchment rang from ~1550 to ~60 m a. s. l. (Fig. 2.4 in Engen-Skaugen et al, 2008a). Annual precipitation in the region is ~2700 mm (Table 2.1 in Engen-Skaugen et al, 2008a). The precipitation is fairly spread through out the year with a dip in spring and summer (Fig. 3.4 in Engen-Skaugen et al, 2008a). In the Norwegian project Regional Climate development under global warming (RegClim <http://regclim.met.no>), annual increase in precipitation for the time period 2071-2100 compared to the time period 1961-1990 is projected to ~5 - 15 % in the area. The largest increase is expected in the autumn (~ 20 - 25 %) Increase is in these regions also projected the remaining seasons (winter: ~15 - 20%; spring: ~10-15 %; summer: ~10 - 15 %) (Iversen et al., 2005). The estimates are based on dynamically downscaling of two global climate model runs following the emission scenario B2. The projections for the period 2020-2050 compared to 1980-1999 following the ECHAM4 GSDIO model and IS92a emission scenario, show similar results for precipitation; largest increase in precipitation in autumn (20-25 %), increase also in winter (~20-30 %) and summer (~10 - 15 %). Reduced precipitation is projected in spring though (~-10 - -5 %) (Førland et al., 2000; Bjørge et al., 2000).

3.12 Viksvatn

Viksvatn is situated the western part of Norway (Fig. 2.1 in Engen-Skaugen et al, 2008a). The size of the catchment is ~500 km² (Table 2.1 in Engen-Skaugen et al, 2008a). The catchment rang from ~1640 to ~150 m a. s. l. (Fig. 2.4 in Engen-Skaugen et al, 2008a). Annual precipitation in the region is ~3800 mm (Table 2.1 in Engen-Skaugen et al, 2008a). The precipitation is distributed through out the year, with an increase during autumn and winter (Fig. 3.17 in Engen-Skaugen et al, 2008a). In the Norwegian project Regional Climate development under global warming (RegClim <http://regclim.met.no>), annual increase in precipitation for the time period 2071-2100 compared to the time period 1961-1990 is projected to ~5 - 15 % in the area. The largest increase is expected in the autumn (~20 - 25 %). Increase is in these regions also projected the remaining seasons (winter: ~10 - 20%; spring: ~10 - 15 %; summer: ~5 - 10 %) (Iversen et al., 2005). The estimates are based on dynamically downscaling of two global climate model runs following the emission scenario B2. P The projections for the period 2020-2050 compared to 1980-1999 following

the ECHAM4 GSDIO model and IS92a emission scenario, show similar results for precipitation; largest increase in precipitation in autumn (~25 - 30 %), increase also in winter (~5 - 10 %) and summer (~20 - 25 %). Minor changes in precipitation is projected in spring though (~0 - 5 %) (Førland et al., 2000; Bjørge et al., 2000).

3.13 Sjudalsvatn

Sjudalsvatn is situated in the high mountain region in the middle of Norway (Fig. 2.1 in Engen-Skaugen et al, 2008a). The size of the catchment is 480 km² (Table 2.1 in Engen-Skaugen et al, 2008a) and the altitude ranges from ~2300 to ~940 m a. s. l. (Fig. 2.4 in Engen-Skaugen et al, 2008a), it drains towards east. Annual precipitation in the region is ~1300 mm (Table 2.1 in Engen-Skaugen et al, 2008a). The precipitation is distributed fairly equal throughout the year with an increase during autumn (Fig. 3.1 in Engen-Skaugen et al, 2008a). In the Norwegian project Regional Climate development under global warming (RegClim <http://regclim.met.no>), annual increase in precipitation for the time period 2071-2100 compared to the time period 1961-1990 is projected to ~5 - 15% in the area. The largest increase is expected in the autumn (~5 - 10 %). Increased precipitation is projected in winter (~5 - 10%) and spring (~5 - 10%), minor reduction in summer (~-5 - 0 %) (Iversen et al., 2005). The estimates from the RegClim project are based on dynamically downscaling of two global climate model runs following the emission scenario B2. The projections for the period 2020-2050 compared to 1980-1999 following the ECHAM4 GSDIO model and IS92a emission scenario, show similar results for precipitation; largest increase in precipitation in autumn (~25 - 30 %), increase also in winter (~5 - 10 %) and summer (~5 - 10 %). Minor changes in precipitation is projected in spring though (~-5 - 0 %) (Førland et al., 2000; Bjørge et al., 2000).

3.14 Orsjoen

Orsjoen is situated in the high mountain region in southern Norway (Fig. 2.1 in Engen-Skaugen et al, 2008a). The size of the catchment is 1177 km² (Table 2.1 in Engen-Skaugen et al, 2008a) it is a rather flat catchment ranging from ~1540 to ~950 m a. s. l. (Fig. 2.5), it drains towards east. Annual precipitation in the region is ~1500 mm (Table 2.1 in Engen-Skaugen et al, 2008a). The precipitation is distributed fairly equal throughout the year with an increase during autumn and winter (Fig. 3.2 in Engen-Skaugen et al, 2008a). In the Norwegian project Regional Climate development under global warming (RegClim <http://regclim.met.no>), annual increase in precipitation for the time period 2071-2100 compared to the time period 1961-1990 is projected to ~5 - 15 % in the area. The largest increase is expected in the autumn (~15 - 20 %) and winter (~15 - 20 %). Increased precipitation is projected also in spring (~10 - 15 %) while reduction is projected in summer (~-15 - -5%) (Iversen et al., 2005). The estimates from the RegClim project are based on dynamically downscaling of two global climate model runs following the emission scenario B2. The projections for the period 2020-2050 compared to 1980-1999 following the ECHAM4 GSDIO model and IS92a emission scenario, show largest increase in precipitation in autumn (~20 - 25 %). Increased precipitation is here also projected for summer (~5 - 15 %), while minor changes are projected for winter (~0 - 5 %) and spring (~-5 - -5 %) (Førland et al., 2000; Bjørge et al., 2000).

3.15 Møsvatn

Møsvatn is situated in the high mountain regions of southern Norway (Fig. 2.1 in Engen-Skaugen et al, 2008a). The size of the catchment is ~1500 km² (Table 2.1 in Engen-Skaugen et al, 2008a) the catchment rang from ~1630 to ~920 m a. s. l. (Fig. 2.5 in Engen-Skaugen et al, 2008a). Annual precipitation in the region is ~1650 mm (Table 2.1 in Engen-Skaugen et al, 2008a). The precipitation is distributed fairly equal throughout the year with an increae in autumn and winter (Fig. 3.23 in Engen-Skaugen et al, 2008a). In the Norwegian project Regional Climate development under global warming (RegClim <http://regclim.met.no>), annual increase in precipitation for the time period 2071-2100 compared to the time period 1961-1990 is projected to ~5 - 15 % in the area. The largest increase is expected in winter (~15 - 20 %) and autumn (~10 - 15 %). Increased precipitation is projected also in spring (~10 - 15 %) while reduction is projected in summer (~-15 - -5%) (Iversen et al., 2005). The estimates are based on dynamically downscaling of two global climate model runs following the emission scenario B2. The projections for the period 2020-2050

compared to 1980-1999 following the ECHAM4 GSDIO model and IS92a emission scenario, show largest increase in precipitation in autumn (~15 - 25 %). Increased precipitation is here also projected for summer (~5 - 15 %), while minor changes are projected for winter (~0 - 5 %) and spring (~-5 - -5 %) (Førland et al., 2000; Bjørge et al., 2000).

3.16 Hølen

Hølen is situated in the western part of Norway (Fig. 2.1 in Engen-Skaugen et al, 2008a). The size of the catchment is ~230 km² (Table 2.1 in Engen-Skaugen et al, 2008a). The catchment rang from ~1700 to ~120 m a. s. l. (Fig. 2.5 in Engen-Skaugen et al, 2008a). Annual precipitation in the region is ~2600 mm (Table 2.1 in Engen-Skaugen et al, 2008a). The precipitation is distributed through out the year, with an increase during autumn and winter (Fig. 3.16 in Engen-Skaugen et al, 2008a). In the Norwegian project Regional Climate development under global warming (RegClim <http://regclim.met.no>), annual increase in precipitation for the time period 2071-2100 compared to the time period 1961-1990 is projected to ~5 - 15 % in the area. The largest increase is expected in the autumn (~15 - 20 %) and winter (~15 - 20 %). Increased precipitation is projected also in spring (~10 - 15 %) while reduction is projected in summer (~-15 - -5%) (Iversen et al., 2005). The estimates are based on dynamically downscaling of two global climate model runs following the emission scenario B2. The projections for the period 2020-2050 compared to 1980-1999 following the ECHAM4 GSDIO model and IS92a emission scenario show largest increase in precipitation in autumn (~20 - 25 %). Increased precipitation is here also projected for summer (~15 - 20 %), while minor changes are projected for winter (~0 - 5 %) and spring (~0 - 5 %) (Førland et al., 2000; Bjørge et al., 2000).

3.17 Reinsnosvatn

Reinsnosvatn is situated in the western part of Norway (Fig. 2.1 in Engen-Skaugen et al, 2008a). The size of the catchment is ~120 km² (Table 2.1 in Engen-Skaugen et al, 2008a). The catchment rang from ~1600 to ~600 m a. s. l. (Fig. 2.5 in Engen-Skaugen et al, 2008a). Annual precipitation in the region is ~3100 mm (Table 2.1 in Engen-Skaugen et al, 2008a). The precipitation is distributed through out the year, with an increase during autumn and winter (Fig. 3.15 in Engen-Skaugen et al, 2008a). In the Norwegian project Regional Climate development under global warming (RegClim <http://regclim.met.no>), annual increase in precipitation for the time period 2071-2100 compared to the time period 1961-1990 is projected to ~5 - 15 % in the area. The largest increase is expected in the autumn (~15 - 20 %). Increase in precipitation is also projected in winter (~10 - 15 %) and spring (~10 - 15 %), while decrease in precipitation is projected during summer (~-15 - -5%) (Iversen et al., 2005). The estimates are based on dynamically downscaling of two global climate model runs following the emission scenario B2. The projections for the period 2020-2050 compared to 1980-1999 following the ECHAM4 GSDIO model and IS92a emission scenario, show largest increase in precipitation in autumn (~25 - 30 %). Increased precipitation is here also projected for summer (~15 - 20 %), while minor changes are projected for winter (~0 - 5 %) and spring (~0 - 5 %) (Førland et al., 2000; Bjørge et al., 2000).

3.18 Stordalsvatn

Stordalsvatn is situated in the western part of Norway (Fig. 2.1 in Engen-Skaugen et al, 2008a). The size of the catchment is ~130 km² (Table 2.1 in Engen-Skaugen et al, 2008a). The catchment rang from ~1250 to ~50 m a. s. l. (Fig. 2.5 in Engen-Skaugen et al, 2008a). Annual precipitation in the region is ~4250 mm (Table 2.1 in Engen-Skaugen et al, 2008a). The precipitation is distributed through out the year, with an increase during autumn and winter (Fig. 3.14 in Engen-Skaugen et al, 2008a). In the Norwegian project Regional Climate development under global warming (RegClim <http://regclim.met.no>), annual increase in precipitation for the time period 2071-2100 compared to the time period 1961-1990 is projected to ~5 - 15 % in the area. The largest increase is expected in the autumn (~25 - 30 %), increased precipitation is projected in winter (~15 - 20 %) and spring (~15 - 20 %) as well. Decrease in precipitation is projected during summer (~-5 - -15%) (Iversen et al., 2005). The estimates are based on dynamically downscaling of two global climate model runs following the emission scenario B2. The projections for the period 2020-2050 compared to 1980-1999 following the ECHAM4 GSDIO model and IS92a emission scenario, show

largest increase in precipitation in autumn (~25 - 30 %). Increased precipitation is here also projected for summer (~20 - 25 %), while minor changes are projected for winter (~0 - 5 %) and spring (~0 - 5 %) (Førland et al., 2000; Bjørge et al., 2000).

3.19 Gjerstad

Gjerstad is situated in near the coast in south-eastern Norway (Fig. 2.1 in Engen-Skaugen et al, 2008a). The size of the catchment is 236 km² (Table 2.1 in Engen-Skaugen et al, 2008a) it is a low laying catchment ~660 to ~80 m a. s. l. (Fig. 2.6 in Engen-Skaugen et al, 2008a), it drains southwards. Annual precipitation in the region is ~1400 mm (Table 2.1 in Engen-Skaugen et al, 2008a). The precipitation is distributed fairly equal throughout the year with increase during autumn and winter (Fig. 3.3 in Engen-Skaugen et al, 2008a). In the Norwegian project Regional Climate development under global warming (RegClim <http://regclim.met.no>), annual increase in precipitation for the time period 2071-2100 compared to the time period 1961-1990 is projected to ~5 - 15 % in the area. The largest increase is expected in the spring (~15-20 %). Increased precipitation is projected in autumn (~10 - 15 %) and winter (~10 - 15 %) as well. Decrease in precipitation is projected during summer (~-15 - -5%) (Iversen et al., 2005). The estimates are based on dynamically downscaling of two global climate model runs following the emission scenario B2. The projections for the period 2020-2050 compared to 1980-1999 following the ECHAM4 GSDIO model and IS92a emission scenario, show increased precipitation in winter (~15 - 20 %) while minor changes are projected the other seasons (spring and summer: ~-5 - 0 %; autumn: ~0 - 5 %) (Førland et al., 2000; Bjørge et al., 2000).

3.20 Austenå

Austenå is situated in southern Norway (Fig. 2.1 in Engen-Skaugen et al, 2008a). The size of the catchment is ~280 km² (Table 2.1 in Engen-Skaugen et al, 2008a) the catchment rang from ~1000 to ~270 m a. s. l. (Fig. 2.6 in Engen-Skaugen et al, 2008a). Annual precipitation in the region is ~1800 mm (Table 2.1 in Engen-Skaugen et al, 2008a). The precipitation is distributed fairly equal throughout the year with an increase in autumn (Fig. 3.25 in Engen-Skaugen et al, 2008a). In the Norwegian project Regional Climate development under global warming (RegClim, <http://regclim.met.no>), annual increase in precipitation for the time period 2071-2100 compared to the time period 1961-1990 is projected to ~-5 - 5% in the area. The largest increase is expected in winter (~15 - 20 %). Increased precipitation is projected also for spring (~10 - 20 %) and autumn (~5 - 10%). Decrease in precipitation is projected for summer (~-15 - -5%) (Iversen et al., 2005). The estimates are based on dynamically downscaling of two global climate model runs following the emission scenario B2. The projections for the period 2020-2050 compared to 1980-1999 following the ECHAM4 GSDIO model and IS92a emission scenario, show increased precipitation in winter (~10 - 15 %) while minor changes are projected the other seasons (spring: ~-5 - 0 %; summer and autumn: ~0 - 5 %) (Førland et al., 2000; Bjørge et al., 2000).

3.21 Flaksvatn

Flaksvatn is situated in southern Norway (Fig. 2.1 in Engen-Skaugen et al, 2008a). The size of the catchment is ~1780 km² (Table 2.1 in Engen-Skaugen et al, 2008a) the catchment rang from ~1000 to ~35 m a. s. l. (Fig. 2.6 in Engen-Skaugen et al, 2008a). Annual precipitation in the region is ~1650 mm (Table 2.1 in Engen-Skaugen et al, 2008a). The precipitation is distributed fairly equal throughout the year with an increase in autumn (Fig. 3.24 in Engen-Skaugen et al, 2008a). In the Norwegian project Regional Climate development under global warming (RegClim, <http://regclim.met.no>), annual increase in precipitation for the time period 2071-2100 compared to the time period 1961-1990 is projected to ~5 - 15 % in the area. The largest increase is expected in winter (~15 - 20 %). Increased precipitation is projected also for spring (~10 - 20 %) and autumn (~5 - 10%). Decrease in precipitation is projected for summer (~-15 - -5%) (Iversen et al., 2005). The estimates are based on dynamically downscaling of two global climate model runs following the emission scenario B2. The projections for the period 2020-2050 compared to 1980-1999 following the ECHAM4 GSDIO model and IS92a emission scenario, show increased precipitation in winter (~10 - 15 %) while minor changes are projected the other seasons (spring: ~-5 - 0 %; summer and autumn: ~0 - 5 %) (Førland et al., 2000; Bjørge et al., 2000).

3.22 Sandvatn

Sandvatn is situated in the south-western part of Norway (Fig. 2.1 in Engen-Skaugen et al, 2008a). The size of the catchment is ~ 27 km² (Table 2.1 in Engen-Skaugen et al, 2008a). The catchment altitude rang from ~ 630 to ~320 m a. s. l. (Fig. 2.6 in Engen-Skaugen et al, 2008a). Annual precipitation in the region is ~2600 mm (Table 2.1 in Engen-Skaugen et al, 2008a). Most of the precipitation falls in autumn (Fig. 3.12 in Engen-Skaugen et al, 2008a). In the Norwegian project Regional Climate development under global warming (RegClim <http://regclim.met.no>), annual increase in precipitation for the time period 2071-2100 compared to the time period 1961-1990 is projected to ~15 – 20 % in the area. Largest increase is expected in the autumn (~20-25 %), winter (~20-25 %) and spring (~20-25 %). Minor changes in precipitation is projected during summer (~-5 - 10%) (Iversen et al., 2005). The estimates are based on dynamically downscaling of two global climate model runs following the emission scenario B2. The projections for the period 2020-2050 compared to 1980-1999 following the ECHAM4 GSDIO model and IS92a emission scenario, show increased precipitation in winter (~10 - 15 %), summer (~15 - 20 %) and autumn (~10 - 15 %). Minor changes are projected in spring (-5 – 0 %) (Førland et al., 2000; Bjørge et al., 2000).

3.23 Årdal

Årdal is situated in the south-western part of Norway (Fig. 2.1 in Engen-Skaugen et al, 2008a). The catchment size is ~77 km² (Table 2.1 in Engen-Skaugen et al, 2008a). The catchments altitude rang from ~731 to ~ 110 m a. s. l. (Fig. 2.6 in Engen-Skaugen et al, 2008a). Annual precipitation in the region is ~3150 mm (Table 2.1 in Engen-Skaugen et al, 2008a). The precipitation is spread through out the year, the largest rainfall comes from September until March (Fig. 3.11 in Engen-Skaugen et al, 2008a). In the Norwegian project Regional Climate development under global warming (RegClim <http://regclim.met.no>), annual increase in precipitation for the time period 2071-2100 compared to the time period 1961-1990 is projected to ~15 - 20% in the area. The largest increase is expected in the autumn (~20-25 %), winter (~20-25 %) and spring (~20-25 %). Minor reduction in precipitation is projected in summer (~-5 - 0%) (Iversen et al., 2005). The estimates are based on dynamically downscaling of two global climate model runs following the emission scenario B2. The projections for the period 2020-2050 compared to 1980-1999 following the ECHAM4 GSDIO model and IS92a emission scenario, show increased precipitation in winter (~10 - 15 %), summer (~20 - 25 %) and autumn (~15 - 20 %). Minor changes are projected in spring (0 - 5 %) (Førland et al., 2000; Bjørge et al., 2000).

3.24 Hetland

Hetland is situated in the south-western part of Norway (Fig. 2.1 in Engen-Skaugen et al, 2008a). The size of the catchment is ~ 70 km² (Table 2.1 in Engen-Skaugen et al, 2008a). The catchment rang from ~530 to ~60 m a. s. l. (Fig. 2.6 in Engen-Skaugen et al, 2008a). Annual precipitation in the region is ~2350 mm (Table 2.1 in Engen-Skaugen et al, 2008a). Most of the precipitation falls in autumn (Fig. 3.13 in Engen-Skaugen et al, 2008a). In the Norwegian project Regional Climate development under global warming (RegClim <http://regclim.met.no>), annual increase in precipitation for the time period 2071-2100 compared to the time period 1961-1990 is projected to ~13% in the area. The largest increase is expected in the autumn (~25 - 30 %), winter (~20 - 25 %) and spring (~20-25 %). Minor changes in precipitation is projected during summer (~-5 - 10%) (Iversen et al., 2005). The estimates are based on dynamically downscaling of two global climate model runs following the emission scenario B2. The projections for the period 2020-2050 compared to 1980-1999 following the ECHAM4 GSDIO model and IS92a emission scenario, show increased precipitation in winter (~10 - 15 %), summer (~20 - 25 %) and autumn (~15 - 20 %). Minor changes are projected in spring (0 - 5 %) (Førland et al., 2000; Bjørge et al., 2000).

3.25 Lyse

Lyse is situated south-western part of Norway (Fig. 2.1 in Engen-Skaugen et al, 2008a). The size of the catchment is ~320 km² (Table 2.1 in Engen-Skaugen et al, 2008a) the catchment rang from ~1300 to ~500 m a. s. l. (Fig. 2.6 in Engen-Skaugen et al, 2008a). Annual precipitation in the region is ~4350 mm (Table 2.1 in Engen-Skaugen et al, 2008a). Most of the precipitation falls from September to May (Fig. 3.20 in

Engen-Skaugen et al, 2008a). In the Norwegian project Regional Climate development under global warming (RegClim <http://regclim.met.no>), annual increase in precipitation for the time period 2071-2100 compared to the time period 1961-1990 is projected to ~5 – 15 % in the area. Increased precipitation is projected in autumn (~25 - 30 %), winter (~15 – 20 %) and spring (~15 – 20 %). Minor change in precipitation is projected during summer (~-5 - 0%) (Iversen et al., 2005). The estimates are based on dynamically downscaling of two global climate model runs following the emission scenario B2. The projections for the period 2020-2050 compared to 1980-1999 following the ECHAM4 GSDIO model and IS92a emission scenario, show increased precipitation in winter (~ 5 - 10 %), summer (~20 - 25 %) and autumn (~20 - 25 %). Minor changes are projected in spring (0 - 5 %) (Førland et al., 2000; Bjørge et al., 2000).

References

- Engen-Skaugen, T., Benestad, R. and Førland, E.J., 2008a, Empirically downscaled precipitation and temperature representing Norwegian catchments, met.no Report No 23 a/2008.
- Engen-Skaugen, T., Benestad, R. and Førland, E.J., 2008b, Results from ESD analyses on temperature representing twenty-five Norwegian catchments, met.no Report No 23 b/2008.
- Bjørge, D., Haugen, J.E. and Nordeng, T.E., 2000, Future climate in Norway. DNMI Research Report 103, Norwegian Meteorological Institute, Oslo
- Førland, E.J., Roald, L.A., Tveito O.E. and Hanssen-Bauer, I., 2000, Past and future variations in climate and runoff in Norway, DNMI Report no. 19/00, Norwegian Meteorological Institute, Oslo
- Iversen, T., Benestad, R., Haugen, J.E., Kirkevåg, A., Sorteberg, A., Debernard, J., Grønås, S., Hanssen-Bauer, I., Kvamstø, N.G., Martinsen, E.A., Engen-Skaugen, T., 2005, Norges klima om 100 år, Usikkerhet og risiko, Brosjyre 3 i prosjektet RegClim (<http://regclim.met.no>).